Reduced generation of lung tissue–resident memory T cells during infancy

Kyra D. Zens,[1,2] Jun Kui Chen,[1] Rebecca S. Guyer,[1] Felix L. Wu,[1] Filip Cvetkovski,[1,2] Michelle Miron,[1,2] and Donna L. Farber[1,2,3]

[1]Columbia Center for Translational Immunology, [2]Department of Microbiology and Immunology, and [3]Department of Surgery, Columbia University Medical Center, New York, NY

Infants suffer disproportionately from respiratory infections and generate reduced vaccine responses compared with adults, although the underlying mechanisms remain unclear. In adult mice, lung-localized, tissue-resident memory T cells (TRMs) mediate optimal protection to respiratory pathogens, and we hypothesized that reduced protection in infancy could be due to impaired establishment of lung TRM. Using an infant mouse model, we demonstrate generation of lung-homing, virus-specific T effectors after influenza infection or live-attenuated vaccination, similar to adults. However, infection during infancy generated markedly fewer lung TRMs, and heterosubtypic protection was reduced compared with adults. Impaired TRM establishment was infant–T cell intrinsic, and infant effectors displayed distinct transcriptional profiles enriched for T-bet–regulated genes. Notably, mouse and human infant T cells exhibited increased T-bet expression after activation, and reduction of T-bet levels in infant mice enhanced lung TRM establishment. Our findings reveal that infant T cells are intrinsically programmed for short-term responses, and targeting key regulators could promote long-term, tissue-targeted protection at this critical life stage.

INTRODUCTION

Infants exhibit increased morbidity and mortality after respiratory infections and experience more repeat infections compared with older children and adults, suggesting impaired protective immunity. The worse outcome for infants in response to infection and their limited or delayed response to vaccines (Siegrist, 2007) have been attributed to the immaturity of immune responses and to T lymphocytes, in particular, which coordinate adaptive immunity (PrabhuDas et al., 2011). Although differences in T cell subset composition and cytokine profile between infant and adult T cells have been described (Lewis et al., 1991; Gibbons et al., 2014; Thome et al., 2016), the basic mechanisms underlying the regulation of infant T cell responses, including their functional differentiation, localization, and maintenance in response to infection remain undefined. There is a critical need for new insights into infant immune responses to both promote protection in response to infection and maximize efficacy of the multiple vaccines administered in early life.

Effective clearance of respiratory pathogens is coupled to establishment of lung-localized effector and memory T cells. In adult mouse models, lung-localized Th1 effector cells producing IFN-γ are important for directing clearance of primary influenza infection (Graham et al., 1993, 1994). We previously showed that populations of $CD4^+$ and $CD8^+$ lung tissue–resident memory T cells (TRM) are generated in response to influenza infection or i.n. administration of live-attenuated influenza vaccine (LAIV) in mice and that these cells mediate rapid, in situ protective responses to secondary viral challenge (Teijaro et al., 2011; Turner et al., 2014; Zens et al., 2016). In humans, influenza-specific $CD4^+$ and $CD8^+$ T cells with TRM phenotypes have been identified within lung tissue (de Bree et al., 2005; Purwar et al., 2011; Turner et al., 2014), and TRM-phenotype cells comprise the majority of memory T cells in diverse human tissues (Sathaliyawala et al., 2013; Thome et al., 2014). The robust protection mediated by TRM in the lungs and their predominance within multiple tissue sites (Masopust et al., 2001; Wakim et al., 2010; Jiang et al., 2012; Shin and Iwasaki, 2012) suggests that TRMs are an important target for promoting antiviral immunity by vaccines and immunotherapies.

The generation of tissue-localized T cell responses within the lung or other sites and the extent to which protective T cell memory and TRMs can be established during infancy have not been well studied. In contrast to adults, most peripheral T cells are naive in early life (Thome et al., 2016) and have distinct patterns of homing receptor expression (Grindebacke et al., 2009; Crespo et al., 2012). Neonatal and infant T cells also exhibit differences in cytokine expression and differentiation after in vitro activation or infection, com-

Correspondence to: Donna L. Farber: df2396@cumc.columbia.edu

Abbreviations used: Ab, antibody; GSEA, gene set enrichment analysis; HA, hemagglutinin; IIV, inactivated influenza vaccine; LAIV, live-attenuated influenza vaccine; logFC, log fold change; NP, nucleoprotein; RIN, RNA integrity number; $TCID_{50}$, 50% tissue culture infective dose; TEM, effector memory T cell; TRM, tissue-resident memory T cell.

The Rockefeller University Press
J. Exp. Med. 2017 Vol. 214 No. 10 2915–2932
https://doi.org/10.1084/jem.20170521

pared with their adult counterparts (Lewis et al., 1986, 1991; Gibbons et al., 2014; Smith et al., 2014). How such differences affect protection and the generation of lasting T cell memory after infection or vaccination is not known.

We hypothesized that reduced protection after infection and decreased vaccine responses observed during infancy could be due to impaired tissue localization of effector T cell responses and/or the establishment of persisting TRM. Using an infant mouse model of influenza infection and vaccination, we found that infants mounted robust, primary, lung-localized $CD4^+$ and $CD8^+$ T cell responses to virus infection and LAIV. However, these cells were inefficiently maintained long term as TRM. In reciprocal transfers, we observed reduced lung TRM establishment after infection by infant, compared with adult, $CD4^+$ T cells in either adult or infant hosts, suggesting T cell–intrinsic differences, rather than the lung environment mediating the distinct infant immune responses. We found distinct transcriptional profiles for infant, compared with adult, T cells after short-term activation in vitro and during the acute response to infection in the lung in vivo, with enhanced expression of T-bet and T-bet–regulated genes in both conditions. Importantly, reducing T-bet expression during infection promoted lung TRM establishment to near-adult levels, indicating that altered differentiation of infant T cells after infection affects TRM formation. These findings provide mechanistic insight into the process of TRM establishment with important implications for promoting vaccine-mediated protection during early life.

RESULTS

Infants generate robust, lung-localized primary T cell responses to influenza infection

We used an infant mouse model to assess tissue-localized immune responses after influenza infection. To accurately recapitulate the immune environment of humans during early life, we elected to use 2-wk-old mice for two reasons: (1) unlike humans, mice are profoundly lymphopenic at birth; and (2) a significant fraction of peripheral T cells in the first week of mouse life have a memory phenotype because of recent homeostatic expansion (Garcia et al., 2000; Le Campion et al., 2002). We assessed T cell populations in the spleen and lungs of mice at different postnatal times and found that, at 2 wk old, the peripheral T cell compartment begins to resemble that of humans in early life (Thome et al., 2016), with increased T cell numbers in the lungs and spleen (Fig. 1 A) exhibiting predominant, naive phenotypes (not depicted).

We infected 2 wk-old, infant mice and 8–16-wk-old adult mice, for comparison, with weight-adjusted, sublethal doses of influenza virus. Throughout the course of the infection, infant mice had similar lung viral burdens as adults, with peak viral loads between days 3 and 5, and the virus was effectively cleared by day 10. However, infants exhibited a slight delay in complete viral clearance (D9 vs. D11) relative to adults (Fig. 1 B). The neutralizing antibody (Ab) titer on day 10 after infection was reduced in infants compared with adults (Fig. 1 C), coincident with the delayed viral clearance.

The primary T cell response in the lung at days 10–15 after infection was similar in infant and adult mice as that assessed by phenotype and by the frequencies of influenza-specific T cells. Overall, there were similar high frequencies (60–80%) of $CD4^+$ and $CD8^+$ T cells exhibiting an effector phenotype ($CD44^+CD62L^{lo}$) in infant and adult lungs, compared with lower frequencies of effector cells in the spleen (30–40%; Fig. 1 D). Moreover, frequencies and total numbers of lung-localized $CD8^+$ T cells specific for influenza virus–immunodominant epitopes, including hemagglutinin (HA), polymerase basic protein 1 (PB1), and nucleoprotein (NP), were similar in infant and adult mice 10–15 d after infection and greatly exceeded the frequencies in adult and infant spleens (Fig. 2 A). Together, these results reveal a robust, primary, influenza-specific T cell response in the lungs of infant mice that is comparable to adult mice, indicating that infant mice are fully competent to mobilize T cell responses to the site of respiratory tract infection.

Although peak T cell responses (D7–15) were similar between infant and adult mice, infant mice displayed a marked reduction in the percentage of lung virus–specific T cells, relative to adults, during the contraction phase of the response that occurs at early times after viral clearance (D16-21; Fig. 2 B). At longer times after infection (6–8 wk), when persisting cells bear phenotypic and functional features of memory T cells (Jelley-Gibbs et al., 2005; Teijaro et al., 2011; Turner et al., 2014), there were reduced frequencies and total numbers of NP-specific $CD8^+$ T cells in mice infected initially as infants, compared with those infected as adults, with biased persistence in lung compared with spleen (Fig. 2, C and D). Taken together, these data demonstrate that infant mice generate lung-localized, virus-specific T cells during acute infection, which correlates with lung viral clearance, but show reduced persistence of virus-specific T cells in the lung at longer times after viral clearance, compared with persisting memory T cells observed in adult mice.

Reduced establishment of lung TRM from infection during infancy

Because of the importance of TRM in long-term protection from repeated influenza infection (Teijaro et al., 2011; Zens et al., 2016), we investigated the generation of persisting lung TRM in mice previously infected as infants (at 2 wk old) compared with those previously infected as adults (at 10–16 wk old). To distinguish circulating T cells from tissue-localized TRM, we used a well-validated, i.v. Ab-labeling technique involving i.v. infusion of fluorescently conjugated anti–T cell antibodies to distinguish between circulating and tissue-resident T cells with the circulating T cells being labeled by i.v. Ab, whereas T cells retained within tissues are protected from Ab binding (Anderson et al., 2012; Turner et al., 2014). "Labeled" T cells, which bind i.v. Ab, and "protected" T cells, which do not, exhibit phenotypic markers of circulating T cells and TRM cells, respectively, and are localized to distinct niches of the lung (Anderson et al., 2012; Turner et al., 2014).

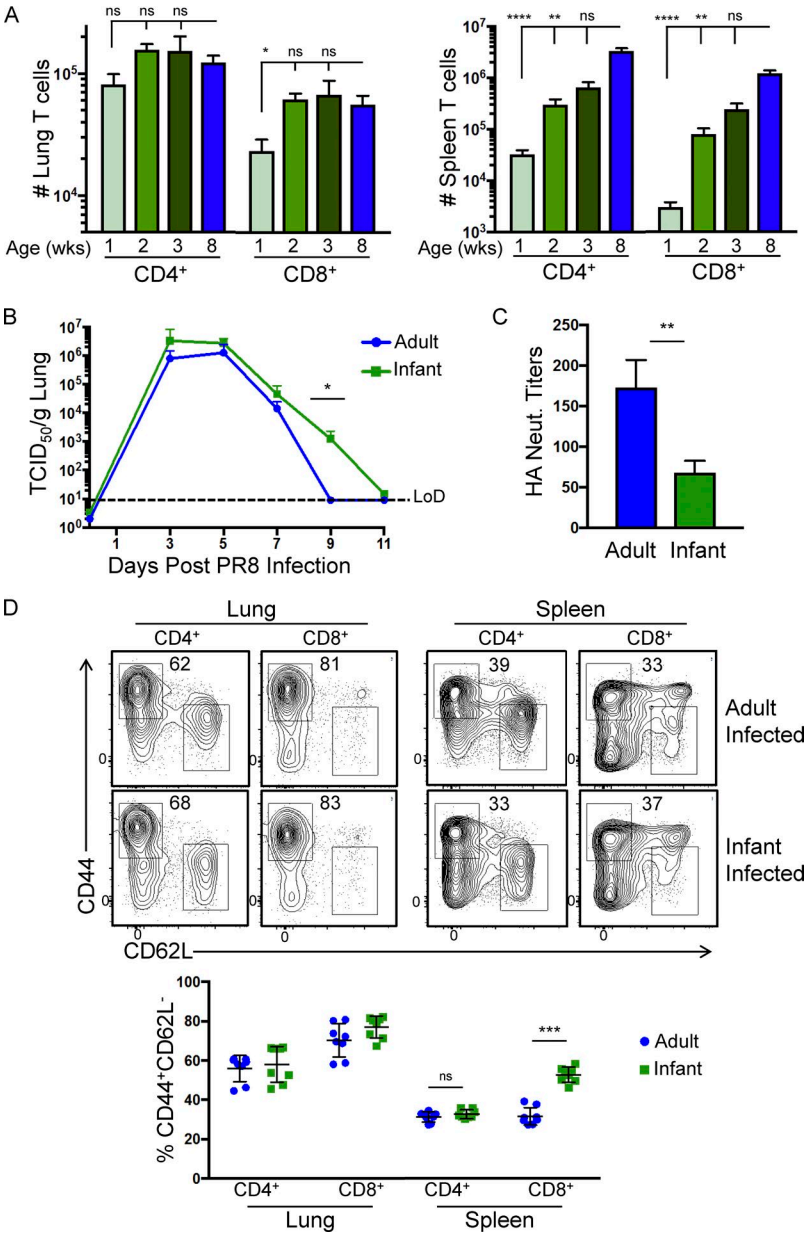

Figure 1. **Primary response to influenza infection in infant and adult mice.** (A) Analysis of T cell numbers at various postnatal ages. Total numbers of lung (left) and spleen (right) $CD4^+$ and $CD8^+$ T cells ± SEM in naive infant mice 1–3 wk old and in adult mice 8 wk old (n = 6–17 mice/group compiled from six independent experiments; significance was determined by one-way ANOVA comparing each infant group to adult controls with Dunn's multiple comparisons test). ns, $P > 0.05$; *, $P < 0.05$; **, $P < 0.01$; ****, $P < 0.0001$. (B) Infant (2 wk old) and adult (10–16 wk old) mice were infected with weight-adjusted, sublethal doses of PR8 influenza, and lung viral titers were assessed at the indicated times. Graph shows kinetics of lung viral clearance in adult and infant mice expressed as $TCID_{50}$/g of lung tissue (±SEM) at the indicated times after infection (n = 3–5 mice per time point, per group compiled from two independent experiments; significance was determined by multiple Student's t tests comparing infant to adult; *, $P < 0.05$). (C) Serum HA neutralizing (Neut.) Ab titers, in hemagglutination inhibition assay units (means ± SEM) to whole PR8 viral particles obtained from adult and infant mice at 10 d after infection (n = 8–10 mice/group compiled from two independent experiments; significance was determined by two-tailed Student's t test with Welch's correction; **, $P < 0.01$). (D) Lung and spleen $CD4^+$ and $CD8^+$ T cells in adult and infant mice 15 d after infection. (Top) Representative plots showing percentages of $CD4^+$ and $CD8^+$ T cells with an effector/memory ($CD44^{hi}CD62L^{lo}$) phenotype (top number). (Bottom) Individual percentages (±SEM) of effector/memory populations (n = 4–8 mice/group compiled from two independent experiments; significance was determined by two-tailed Student's t test with Welch's correction; ns, $P > 0.05$; ***, $P < 0.001$).

In mice previously infected as adults, most lung $CD4^+$ and $CD8^+$T cells (>75%) were protected from i.v. Ab labeling 6 wk after infection, consistent with our previous findings (Turner et al., 2014; Zens et al., 2016). In contrast, in mice previously infected as infants (at 2 wk old), the proportion of protected lung T cells at 6 wk after infection was greatly reduced compared with mice infected as adults (35–45%, on average) and was similar to that observed in uninfected controls (Fig. 3 A). Furthermore, although most NP-specific $CD8^+$ T cells in the lungs of mice infected as adults were protected from i.v. labeling, consistent with localization in the tissue, a significant fraction (25–30%) of NP-specific lung $CD8^+$ T cells in mice previously infected as infants were labeled by i.v. Ab (Fig. 3 B), indicating these cells were circulating. These results indicate that infection during infancy reduces the persistence of total and virus-specific memory T cells in the protected niche of the lung.

We further investigated whether protected lung T cells in infants expressed the canonical TRM marker CD69 on the cell surface, along with CD11a for $CD4^+$ TRM and CD103 for $CD8^+$ TRM (Mueller et al., 2013; Turner and Farber, 2014). Consistent with previous studies, a significant fraction of protected $CD4^+$ and $CD8^+$ T cells in adults were $CD69^+CD11a^+$ (>60% of $CD4^+$) or $CD69^+CD103^+$ (~50% of $CD8^+$). By contrast, in mice previously infected as infants, <50% of protected $CD4^+$T cells and 25% of protected $CD8^+$T cells expressed those TRM phenotypes (Fig. 3 C). Expression of TRM markers in previously infected infants

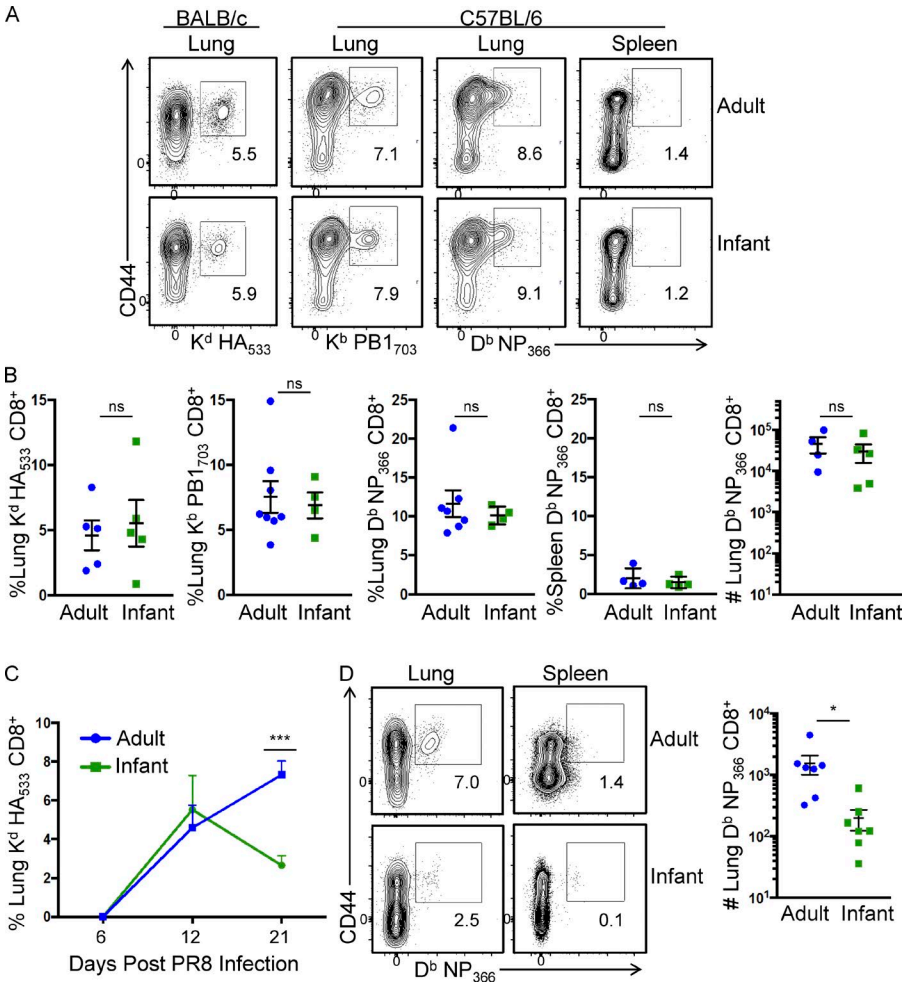

Figure 2. **Comparable primary virus–specific lung T cell responses in infants and adults after influenza infection.** Infant (2 wk old) and adult (10–16 wk old) mice were infected as shown in Fig. 1. (A) Representative plots showing percentages of influenza-specific $CD8^+$ T cells in the lungs and spleens at 12–15 d after infection in adult and infant BALB/c and C57BL/6 mice, as indicated. (Left) Lung $HA_{533-541}$–specific $CD8^+$ T cells; (Middle) Lung $PB1_{703-711}$–specific $CD8^+$ T cells; (Right two columns) Lung and spleen $NP_{366-374}$–specific $CD8^+$ T cells in infected adult and infant mice. (B) Individual percentages of lung or spleen virus-specific $CD8^+$ T cells or total numbers of lung $NP_{366-374}$-specific $CD8^+$ T cells as shown in A for infected infant and adult mice ± SEM (n = 4–8 mice-group compiled from three independent experiments; significance was determined by two-tailed Student's t test with Welch's correction; ns, $P > 0.05$). (C) Frequencies of $HA_{533-541}$–specific lung $CD8^+$ T cell in adult or infant mice at indicated times after infection ± SEM (n = 5 mice/group, representative of two experiments; significance was determined by multiple Student's t tests with Welch's correction; ***, $P < 0.001$). (D) Persistence of influenza-specific $CD8^+$ T cells 6 wk after infection of infant and adult mice. (Left) Representative flow cytometry plots showing frequencies of $NP_{366-374}$–specific $CD8^+$ T cells in lung and spleen. (Right) Absolute numbers of $NP_{366-374}$–specific $CD8^+$T cells (±SEM) in the lungs of mice infected as adults or infants 6 wk previously (n = 7–10 mice/group, compiled from three independent experiments; significance was determined by Student's t test with Welch's correction; *, $P < 0.05$).

was, however, increased compared with uninfected controls (Fig. 3 C), suggesting that TRM generation during infancy is greatly reduced but not completely inhibited. Overall, these findings demonstrate reduced establishment of canonical lung TRM after influenza infection during infancy.

Altered lung-localized protection in mice infected during infancy

To assess whether reduced TRM formation in mice infected initially as infants resulted in decreased protection against heterosubtypic strains later in life, we challenged infant and adult mice infected with PR8 influenza 6 wk previously and naive adults as controls, with the heterosubtypic H3N2 viral strain X31. To further investigate TRM-mediated protection, independent from that mediated by circulating T cells, we treated cohorts of mice throughout infection with the sphingosine 1-phosphate receptor-1 agonist FTY720, which sequesters circulating T cells within the secondary lymphoid tissues and depletes circulating T cells (Chiba et al., 1998; Pinschewer et al., 2000), whereas lung TRM are maintained (Anderson et al., 2014; Turner et al., 2014; Zens et al., 2016).

In PBS-treated cohorts, heterosubtypic challenge of mice previously infected as adults or infants resulted in minimal weight-loss morbidity, compared with primary X31 infection of naive mice, which resulted in significant weight loss during the course of infection (Fig. 4 A). However, mice previously infected as adults exhibited enhanced viral clearance from the lungs by day 5 after challenge compared with mice previously infected as infants although titers in this group were reduced, compared with primary infection controls (Fig. 4 B). These results indicate that infection during infancy results in immunity to heterosubtypic infection, which is reduced in efficacy compared with infections occurring later in life.

In FTY720-treated groups, mice previously infected as infants lost significant weight after heterosubtypic challenge, which was similar to the weight loss of primary infection controls and significantly greater than that observed in mice previously infected as adults (Fig. 4 A). Moreover, the lung

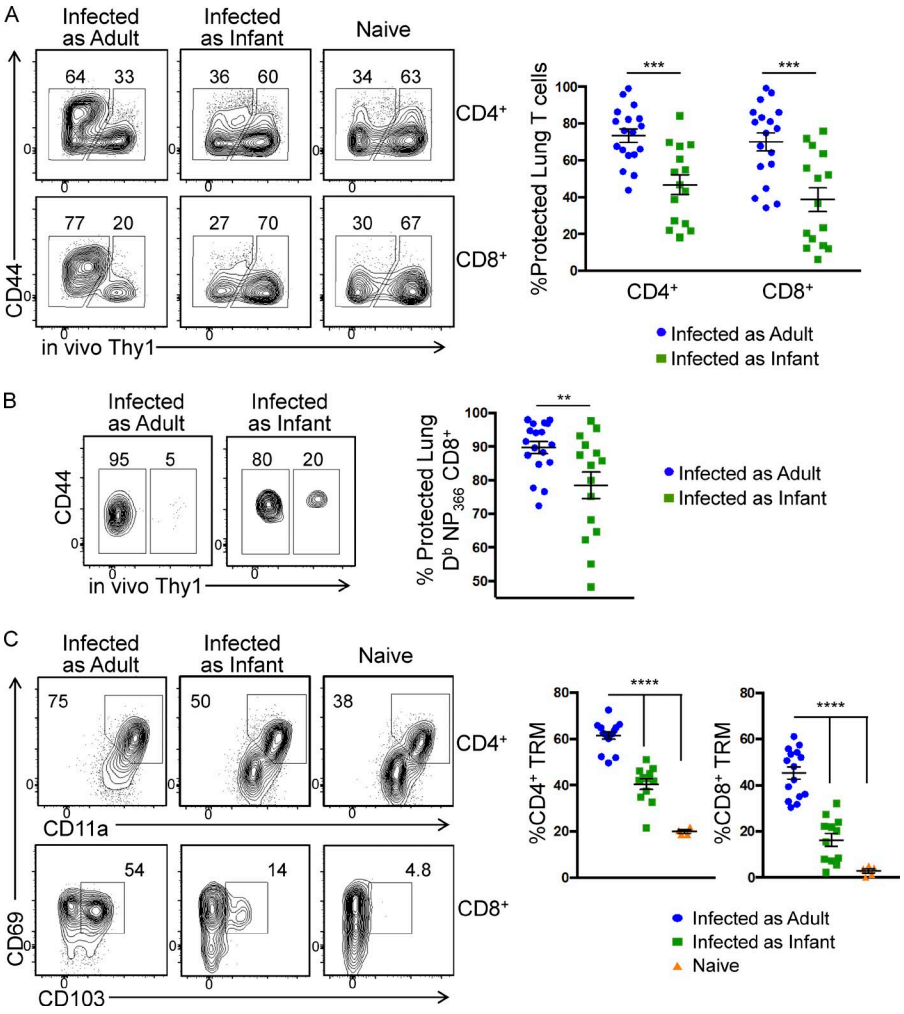

Figure 3. **Infants generate reduced lung TRM compared with adults after influenza infection.** Infant and adult mice were infected with PR8 influenza as in Fig. 1 and lung T cell populations were assessed 6 wk after infection. (A) Lung $CD4^+$ or $CD8^+$ T cells labeled by, or protected from, i.v. anti-Thy1 Abs in mice infected 6 wk previously as infants (2 wk old) or adults (10-16 wk old) or in uninfected (naive) adult controls (10–16 wk old). (Left) Representative flow cytometry plots showing percentages of labeled (right number) and protected (left number) lung $CD4^+$ or $CD8^+$ T cells. (Right) Individual percentages (±SEM) of protected lung $CD4^+$ or $CD8^+$ T cells (n = 15–18 mice/group, compiled from four independent experiments; significance was determined by two-way ANOVA with Holm-Sidak's multiple comparisons test; ***, $P < 0.001$). (B) Lung $NP_{366–374}$–specific memory $CD8^+$ T cells in mice infected 6 wk previously as infants or adults. (Left) Representative flow plots. (Right) Individual percentages of protected lung $NP_{366–374}$–specific $CD8^+$ T cells from previously infected adult or infant mice ± SEM (n = 15–18 mice/group, compiled from four independent experiments; significance was determined by Student's t test with Welch's correction; **, $P < 0.01$). (C) Expression of TRM phenotype markers (CD11a, CD69, CD103) by protected lung $CD4^+$ or $CD8^+$ T cells in mice infected 6 wk previously as infants or adults or in uninfected, naive, adult-littermate controls. (Left) Representative flow plots. (Right) Individual percentages (±SEM) of lung $CD4^+$ TRM ($CD69^+CD11a^+$) or $CD8^+$ TRM ($CD69^+CD103^+$) in mice previously infected as adults or infants compared with uninfected mice (n = 5–15 mice/group, compiled from three independent experiments; significance was determined by two-way ANOVA with Holm-Sidak's multiple comparisons test; ****, $P < 0.0001$).

viral burden 5 d after challenge was similarly increased in naive mice and mice previously infected as infants, compared with mice previously infected as adults (Fig. 4 B). These results demonstrate that FTY720 treatment (reducing circulating T cell responses) reduced the rapid viral clearance and early protection in mice previously infected as infants, whereas the early and enhanced protective response in mice previously infected as adults was preserved. These findings suggest impaired establishment of protective lung TRM after infection in infancy.

Reduced lung TRM establishment in LAIV-vaccinated infants

We previously showed in adult mice that, of the current influenza vaccines, LAIV administered i.n. and inactivated influenza virus (IIV) administered by injection (s.c. or i.p.), only i.n. LAIV promoted generation of lung TRM protective against heterosubtypic infection (Zens et al., 2016). We investigated whether reduced TRM generation in infant, compared with adult, mice was specific to influenza infection or was a generalized defect in overall immune and vaccine responses. After immunization of infant and adult mice i.n. with LAIV or i.p. with IIV, we analyzed lung T cell populations 10 d or 6 wk after vaccination and protection to heterosubtypic challenge. As we previously reported, adult mice exhibited robust primary lung $CD4^+$ and $CD8^+$ effector responses to i.n. LAIV and minimal lung T cell responses to IIV (Fig. 5 A). Infants exhibited similar primary vaccine responses to adults with higher percentages of lung $CD4^+$ and $CD8^+$ effector cells were observed after vaccination with LAIV, compared with IIV (Fig. 5 A). Thus, infants mount comparable primary lung T cell responses as adults to the vaccine formulations.

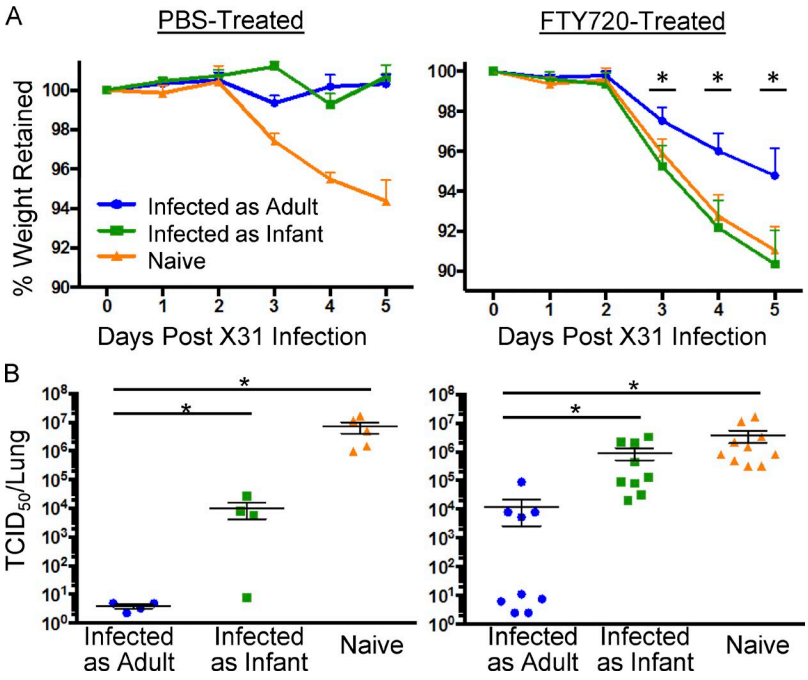

Figure 4. **Reduced lung TRM-mediated heterosubtypic protection in mice previously infected during infancy versus adulthood.** Mice were infected with PR8 influenza as infants (2 wk old) or as adults (10–16 wk old) as in Fig. 2, and 6 wk later, groups were challenged with the heterosubtypic strain X31 strain in the presence of treatment with FTY720 or PBS control. Naive mice were littermate controls of PR8-infected adult mice that were similarly challenged with X31. (A) Morbidity after heterosubtypic challenge expressed as mean percentage of weight retention (±SEM) after infection in mice treated daily with PBS (left) or FTY720 (right; n = 4–9 mice/group compiled from two independent experiments; significance was determined by multiple Student's t tests comparing infected-as-adult to infected-as-infant mice; *, $P < 0.05$). (B) Lung viral titers 5 d after heterosubtypic challenge in mice previously infected as adults or infants as in A. Individual lung viral titers ($TCID_{50}$/lung ± SEM) are shown for mice receiving daily PBS treatment (left) or FTY720 treatment (right; n = 4–9 mice/group, compiled from two independent experiments; significance was determined by one-way ANOVA with Holm-Sidak's multiple comparisons test; *, $P < 0.05$).

At longer times after vaccination, adult mice generated significant frequencies of lung $CD4^+$ and $CD8^+$ TRM (as assessed by CD69 and CD103 expression) after vaccination with LAIV but not IIV (Zens et al., 2016; Fig. 5 B). In contrast, infant mice vaccinated with LAIV or IIV had only low frequencies of persisting lung TRM (Fig. 5 B). TRM-mediated protection to heterosubtypic challenge with PR8 influenza was also assessed in vaccinated mice in the presence of FTY720, as shown in Fig. 4. Infant mice vaccinated with LAIV or IIV and adult mice vaccinated with IIV all lost significantly more weight throughout the course of infection, compared with adult mice vaccinated with LAIV who did not exhibit as extensive weight loss (Fig. 5 C). In terms of lung viral clearance, adults and infants vaccinated with IIV had similarly high lung viral burdens 7 d after infection, whereas adults and infants vaccinated with LAIV had reduced lung viral titers at that time point (Fig. 5 D). These results demonstrate that, although vaccination with LAIV during infancy elicits reduced establishment of lung TRM compared with adults, as observed with influenza infection, some degree of protective lung immune responses was generated by LAIV administration during infancy.

Reduction in lung TRM establishment by infant mice is T cell intrinsic

We investigated whether the reduced generation of lung TRM from influenza infection during infancy was due to the distinct lung environment of infants and/or to intrinsic differences between infant and adult T cells. We focused our mechanistic studies on $CD4^+$ T cells because of their known requirement in generation of memory $CD8^+$ T cells and lung $CD8^+$ TRM formation (Sun and Bevan, 2003; Bevan, 2004; Williams et al., 2006; Laidlaw et al., 2014). We performed reciprocal adoptive transfers of infant- or adult-derived influenza HA-specific $CD4^+$ T cells (HA T cells) to congenic infant or adult recipients to generate four groups: (1) adult HA–adult host (adult to adult), (2) adult HA–infant host (adult to infant), (3) infant HA–adult host (infant to adult), and (4) infant HA–infant host (infant to infant). The resultant groups were subsequently infected with PR8 influenza; primary lung T cell responses were assessed on day 13, and persistence as memory T cells was assessed 6 wk later.

Early after transfer and infection, there were comparable frequencies of infant- and adult-derived HA T cells in both the lungs and mediastinal LN of adult recipients (Fig. 6 A), suggesting that both adult and infant T cells survived adoptive transfer to comparable extents. Similarly, during the peak primary T cell response (day 13) similar percentages of HA T cells were detected in the lungs in all recipient mice (Fig. 6, B and C). At longer times after infection, there were comparable low, but discernable, frequencies of adult HA T cells in the lungs of both adult and infant recipients; however, we did not detect significant populations of persisting, infant-derived HA T cells in the lungs of adult or infant hosts (Fig. 6, B and C). These results demonstrate that, although infant cells migrate to the lung and expand in response to influenza infection, similar to adult cells, they are not efficiently maintained as lung memory T cells regardless of the host environment, indicating a cell-intrinsic basis for reduced TRM generation in infants.

Distinct transcriptional profile of infant and adult lung T cells involving T-bet

We hypothesized that distinct gene expression patterns between adult and infant T cells during the primary response

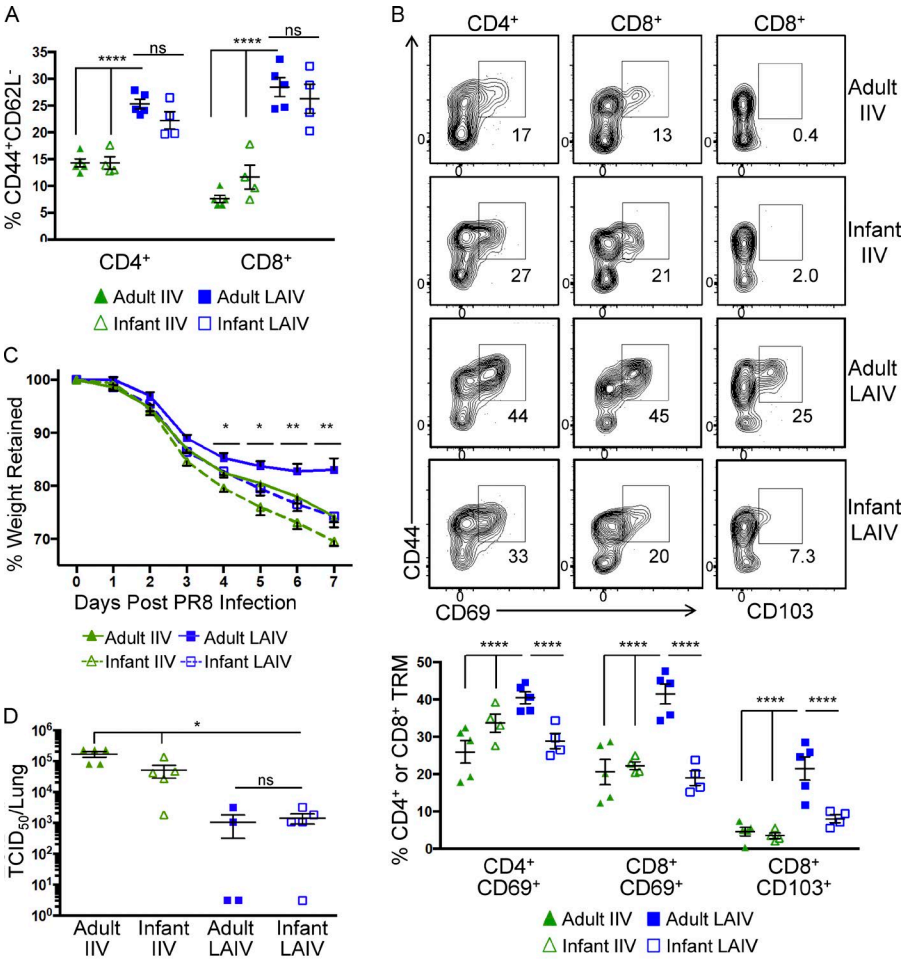

Figure 5. **Reduced TRM generation and TRM-mediated heterosubtypic protection in LAIV-vaccinated infants compared with adults.** Infant and adult mice were vaccinated i.p. with IIV or i.n. with LAIV (littermate controls were used for the different vaccinations) and lung T cell responses were analyzed 10 d or 6 wk later. (A) Frequency of lung effector/memory ($CD44^+CD62L^{lo}$) $CD4^+$ and $CD8^+$ T cells in adult or infant mice vaccinated 10 d prior with IIV or LAIV (individual data ± SEM, n = 4–5 mice/group, representative of two experiments; significance determined by two-way ANOVA with Holm-Sidak's multiple comparisons test; ns, $P > 0.05$; ****, $P < 0.0001$). (B) Lung $CD4^+$ and $CD8^+$ TRM in mice vaccinated 6 wk previously with IIV or LAIV as adults or infants. (Top) Representative flow cytometry plots. (Bottom) Individual frequencies of protected lung $CD4^+$ and $CD8^+$ T cells expressing CD69 or CD103 ± SEM (n = 4–5 mice/group, representative of 2 experiments; significance determined by multiple Student's t tests with Holm-Sidak's comparison correction; ****, $P < 0.0001$). (C) Mice vaccinated as in B were challenged i.n. with the heterosubtypic strain PR8 (H1N1) influenza in the presence of FTY720. Graph shows morbidity expressed as mean percentage weight retention ± SEM (n = 5 mice/group, representative of two experiments; significance determined by multiple Student's t tests comparing adult to infant LAIV vaccinated; *, $P < 0.05$; **, $P < 0.01$). (D) Lung viral titers 7 d after PR8 infection in mice challenged as in C (individual data ± SEM; n = 4–5 mice/group, representative of two experiments; significance determined by one-way ANOVA with Holm-Sidak's multiple comparisons test; ns, $P > 0.05$; *, $P < 0.05$ between IIV- and LAIV-vaccinated groups).

could drive T cell–intrinsic differences in TRM formation. We transferred infant or adult HA T cells to adult congenic hosts, infected them with PR8 influenza as shown in Fig. 6, and sorted infant or adult HA-specific $CD4^+$ T cells (referred to as "HA effectors") from host lungs 13 d later for whole transcriptome profiling by RNA sequencing.

A total of 634 genes were significantly differentially expressed ($P < 0.05$) between infant and adult HA effectors (Fig. 7 A and Tables S1 and S2). Among those, several well-established molecules important for lung tissue homing and retention, including CCR2, CCR5, CXCR6, CCR8, and Itga1 (VLA-1; Dawson et al., 2000; Ray et al., 2004; Richter et al., 2007; Kohlmeier et al., 2008; Morgan et al., 2008; Lee et al., 2011), were consistently up-regulated by infant HA effectors relative to those of adults (Table S1). Expression of transcription factors typically associated with effector T cell differentiation and function, including Blimp1, Id2, and T-bet (Intlekofer et al., 2005; Cannarile et al., 2006; Ji et al., 2011; Yang et al., 2011), were also increased in infant, compared with adult, lung HA effectors (Table S1). Conversely, expression of transcription factors associated with memory T cell generation, including Eomes, Bcl6, and Id3 (Johnston et al., 2009; Banerjee et al., 2010; Ji et al., 2011; Yang et al., 2011) were down-regulated in infant, compared with adult, HA effectors (Table S2).

Ingenuity Pathway Analysis (IPA; Krämer et al., 2014) revealed STAT4 and its major target T-bet (Thieu et al., 2008) as predicted, upstream, positive transcriptional regulators of the genes differentially expressed between infant and adult HA effectors (Fig. 7 B). To assess whether either of these or other pathways were up-regulated in infant T cells early after activation, we performed whole transcriptome profiling of infant and adult polyclonal naive ($CD44^{lo}$) $CD4^+$ T cells after short-term activation in vitro with anti–CD3/CD28 Abs for

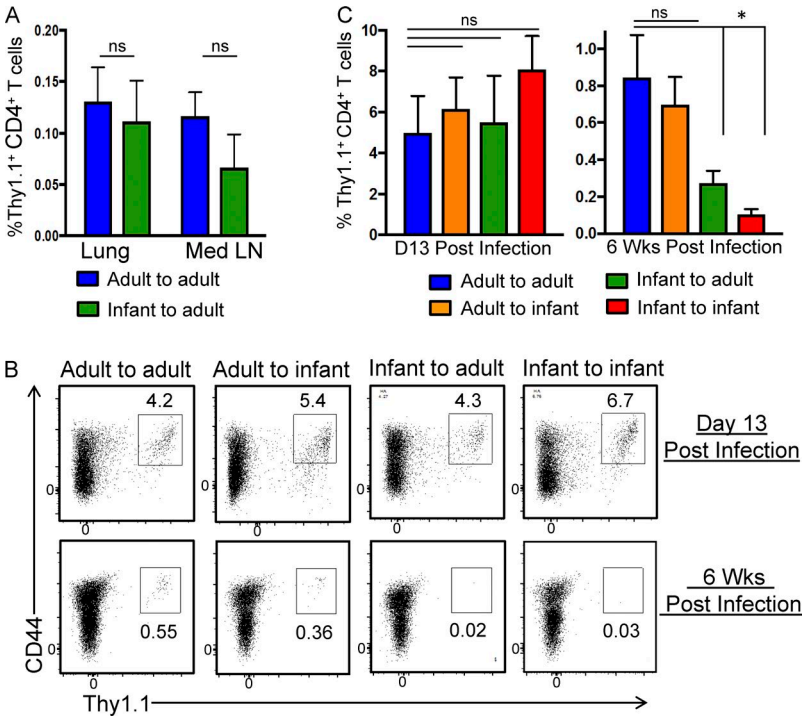

Figure 6. **Reduced lung TRM generation by infants is intrinsic to T cells.** Influenza HA–specific CD4+ T cells isolated from adult or infant TS1-transgenic mice (Thy1.1+) were transferred to adult or infant congenic hosts, respectively, resulting in four groups ([1] adult to adult; [2] adult to infant; [3] infant to adult; and [4] infant to infant) which were subsequently infected with PR8 influenza and assessed 72 h (A), 13 d (B), or 6 wk (C) after infection. (A) Mean frequencies (±SEM) of transferred adult or infant HA-specific T cells (Thy1.1+) in the lungs or mediastinal LNs (Med LN) of adult recipient mice 72 h after infection (n = 10–15 mice/group compiled from three independent experiments; significance was determined by Student's t test with Welch's correction; ns, $P > 0.05$). (B) Representative flow cytometry plots with frequencies of transferred adult or infant HA-specific T cells (Thy1.1+) in the lungs of infant or adult recipient mice 13 d (top row) or 6 wk (bottom row) after infection. (C) Mean frequencies (±SEM) of transferred adult or infant, HA-specific T cells (Thy1.1+) in the lungs of infant or adult recipient mice 13 d (left) or 6 wk (right) after infection (n = 4–11 mice/group, per time point, compiled from six independent experiments; significance was determined by one-way ANOVA with a Holm-Sidak's multiple comparisons test; ns, $P > 0.05$; *, $P < 0.05$).

24 h (Tables S3 and S4). Similar to the differential gene expression data of lung-homing effector cells, T-bet was among the top predicted, upstream regulators of short-term, activated, infant CD4+ T cells by IPA and the only transcriptional regulator present in both data sets with a similar direction of expression (Fig. 7, B and C). Gene Ontology (GO) analysis demonstrated an enrichment for cellular processes associated with cellular replication and proliferation by short-term–activated infant, compared with adult, CD4+ T cells (Table S5). These results suggest enhanced proliferation and differentiation of infant T cells relative to adult cells initiated in the early phases of activation.

To further evaluate a role for T-bet in the regulation of this differentially expressed gene profile, we compared genes differentially expressed between infant and adult HA effectors (634 total) to a list of genes found to be significantly positively or negatively regulated by T-bet in an independent study (430 total; Zhu et al., 2012). There was a substantial degree of overlap between the infant, versus adult, HA effectors gene set and T-bet–regulated genes, with 12% of genes represented in the T-bet–regulated set (Fig. 7, A and D; and Tables S1 and S2). (A similar proportion (~10%) of genes differentially expressed between in vitro–activated infant and adult CD4+ T cells were present in the T-bet–regulated set [Tables S3 and S4]). Gene set enrichment analysis (Subramanian et al., 2005) was applied to the ranked genes to determine whether the direction of gene expression in infant HA effectors was consistent with up-regulated T-bet expression. GSEA revealed a strong correlation ($P < 0.0001$) between genes up-regulated in infant HA effectors with genes known to be positively regulated by T-bet; genes known to be negatively regulated by T-bet were also down-regulated in infant HA effectors, relative to adult (Fig. 7 D). Together these results provide evidence that enhanced T-bet expression may be a key regulator of the distinct differentiation of infant, compared with adult, effector T cells.

Increased T-bet expression in mouse and human, infant T cells

We evaluated T-bet expression by flow cytometry in infant and adult CD4+ T cells before and after activation both in vitro and in vivo. Activation of mouse, infant, naive ($CD44^{lo}$) CD4+ T cells in vitro resulted in augmented T-bet expression with increased kinetics compared with adult, naive CD4+T cells, although levels were comparable by 72 h after stimulation (Fig. 8 A). Similarly, in humans, a greater percentage of infant cells sustained high levels of T-bet relative to adult-derived cells (Fig. 8 B). In vivo, we assessed T-bet expression by infant and adult HA T cells adoptively transferred to infant or adult congenic hosts, which were subsequently infected with influenza. At 13 d after infection, a greater percentage of infant cells expressed T-bet compared with adult cells. This enhanced expression of T-bet was further independent of the host environment with comparable percentages of $T\text{-}bet^{hi}$, infant, HA-specific T cells in both infant and adult hosts (Fig. 8 C), suggesting that enhanced T-bet expression occurs in a cell-intrinsic manner.

For CD8+ T cells, expression of T-bet is inversely correlated with the expression of CD127 (Intlekofer et al., 2007; Joshi et al., 2007; Knox et al., 2014), the α subunit of the IL-7

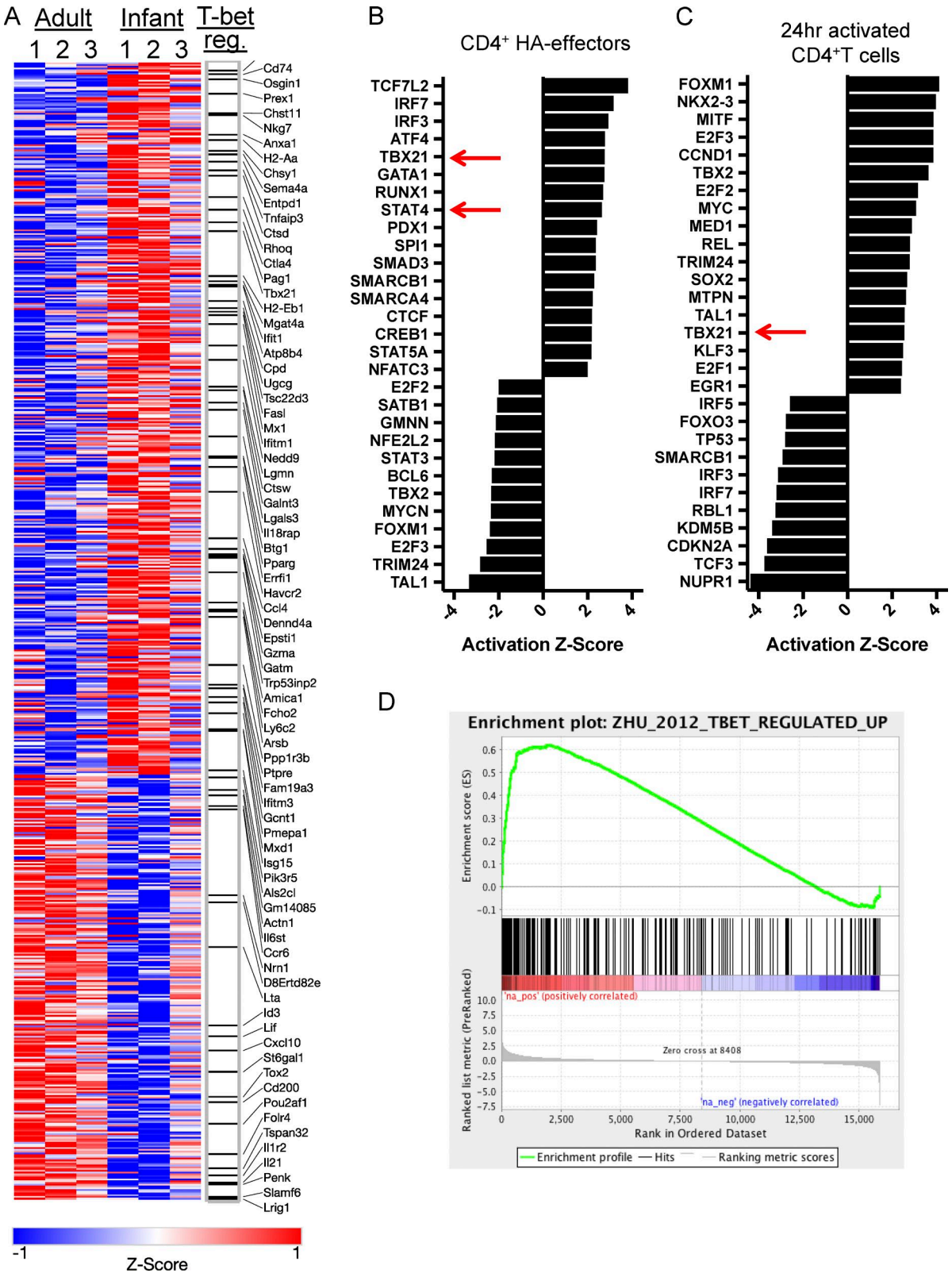

Figure 7. **Gene expression analysis of infant versus adult lung CD4 effectors reveals a T-bet signature.** Influenza HA-specific CD4+ T cells isolated from infant or adult TS1 mice (Thy1.1+) were transferred to adult congenic hosts, which were subsequently infected with PR8 influenza as in Fig. 6, and lung Thy1.1+ cells ("HA effectors") were sorted 13 d later for whole-transcriptome profiling by RNA-Seq. (A) Heat map of genes (634 total) significantly (P <

receptor, a well-described T cell survival factor (Schluns et al., 2000; Kaech et al., 2003), with high levels of T-bet driving the generation of terminally differentiated, short-lived effector cells (Intlekofer et al., 2007; Joshi et al., 2007). We therefore measured CD127 expression during the course of influenza infection in both adult and infant mice. At 6, 12, and 21 d after infection, CD127 expression levels were significantly higher in adult lung $CD4^+$ T cells compared with infant cells (Fig. 8 D), suggesting that enhanced T-bet expression in infant T cells might be associated with reduced capacity to respond to survival factors.

Reduced T-bet expression promotes TRM generation in infants

Our results suggested that increased T-bet expression by infant T cells after activation could bias toward generation of short-lived effector cells, inhibiting development of memory T cells and persistence of lung-homing effector cells as TRMs. To test whether specific reduction of T-bet expression by infant T cells could enable generation of lung TRM, we used infant mice heterozygous for T-bet to effectively "modulate" T-bet expression. Because T-bet expression is codominant, deletion of a single allele reduces expression on a per-cell basis. We infected infant T-$bet^{+/+}$ (WT) and T-$bet^{+/-}$ mice, along with T-$bet^{+/-}$ and WT adult controls, with PR8 influenza and assessed lung TRM generation 6–8 wk later.

At 6 wk after infection, T-$bet^{+/-}$ mice previously infected as infants had increased numbers of protected lung $CD4^+$ and $CD8^+$ T cells, compared with WT mice infected as infants, and similar numbers of protected lung T cell as WT and T-$bet^{+/-}$ mice infected as adults (Fig. 9 A). Similarly, in T-$bet^{+/-}$ mice previously infected as infants, most protected lung $CD4^+$ (∼50–60%) and $CD8^+$ T cells (40–50%) expressed canonical $CD4^+$ and $CD8^+$ TRM markers, similar to WT and T-$bet^{+/-}$ mice previously infected as adults (Fig. 9 B). By contrast, only 40% of protected $CD4^+$ T cells and 20% of protected $CD8^+$ T cells in WT mice infected as infants expressed those markers (Fig. 9 B). In addition, we confirmed that T-bet expression was reduced in both naive $CD4^+$ and $CD8^+$ T cells and TRMs in T-$bet^{+/-}$ infant memory mice compared with WT adult memory mice (Fig. 9 C). These results demonstrate that reducing T-bet expression in infant T cells results in TRM establishment similar to that in WT adults, suggesting that dysregulation of T-bet by infants during the primary response to infection results in the reduced generation of lung TRM.

DISCUSSION

Infants are highly susceptible to respiratory viral pathogens; however, the state of infant lung immune responses during homeostasis and infection is poorly understood. Using an infant mouse model that recapitulates the state of human early life immunity, we provide mechanistic insights into the regulation, differentiation, and maintenance of infant lung T cell responses during respiratory virus infection and vaccination. We demonstrated that influenza infection (or i.n. vaccination) of infant mice results in effective mobilization of $CD4^+$ and $CD8^+$ T cell responses in the lung and viral clearance but inefficient establishment of lung TRMs and in situ protective immunity. Reduced TRM differentiation by infant lung-homing T cells was due to a distinct transcriptional profile indicative of enhanced proliferation and increased expression of T-bet–regulated genes. This enhanced expression of T-bet correlated with reduced expression of the survival factor CD127 by infant T cells. Significantly, down-modulation of T-bet expression augmented TRM development in infant mice. Together, our findings suggest that infant T cells are intrinsically programmed for short-term pathogen clearance rather than long-term maintenance and that targeting a key regulator can enable long-term immunity at this critical life stage.

We demonstrated that infant mice generate influenza-specific, lung-homing T cell responses after respiratory infection, which are qualitatively and quantitatively similar to responses observed in adult mice. That result was confirmed in different strains of mice for T cells specific for multiple influenza epitopes and is consistent with studies in humans showing mobilization of T cells with effector phenotypes in the airways of infants with respiratory infections (Connors et al., 2016). Previous studies of respiratory infection in neonatal mice (<1 wk old) have reported delayed and quantitatively reduced $CD8^+$ T cell responses with altered homing patterns relative to adults (You et al., 2008; Lines et al., 2010). However, neonatal mice are profoundly lymphopenic, resulting in extensive T cell homeostatic expansion in the early neonatal period (Min et al., 2003; Schönland et al., 2003), which can affect T cell differentiation and function (Surh and Sprent, 2000, 2008). Mice at 2 wk of age were chosen specifically to be representative of human infants who are born replete with a full T cell complement.

Developing protective immunity to respiratory infections is coupled to the generation of lung TRMs (Teijaro

0.05) differentially expressed between adult and infant lung HA effectors showing relative gene expression from three independent isolates (designated 1, 2, and 3) of adult and infant HA effectors pooled from 5–10 mice/experiment. (Farthest right column) Genes within the heat map ($n = 78$) regulated by the transcription factor T-bet ("T-bet reg."). (B) Top predicted, upstream transcriptional regulators, determined using the IPA tool, based on differential gene expression patterns between adult and infant lung HA effectors as displayed in A. Top 30 upstream regulators as assessed by P value, sorted by z-score. Arrows indicate values for T-bet and STAT4. (C) Top IPA-predicted upstream transcriptional regulators based on differential gene expression patterns between adult and infant, spleen-derived, naive ($CD44^{lo}$) $CD4^+$ T cells stimulated with anti–CD3 and anti–CD28 for 24 h (see Materials and methods). Top 30 transcriptional regulators, as assessed by P value, sorted by z-score. Arrow indicates values for T-bet. Data are representative of gene expression from two independent isolations of adult and infant spleen $CD44^{lo}CD4^+$ T cells pooled from 2–10 mice/experiment. (D) GSEA comparing genes significantly differentially expressed between adult and infant lung HA effectors as in A with independently identified T-bet–regulated genes.

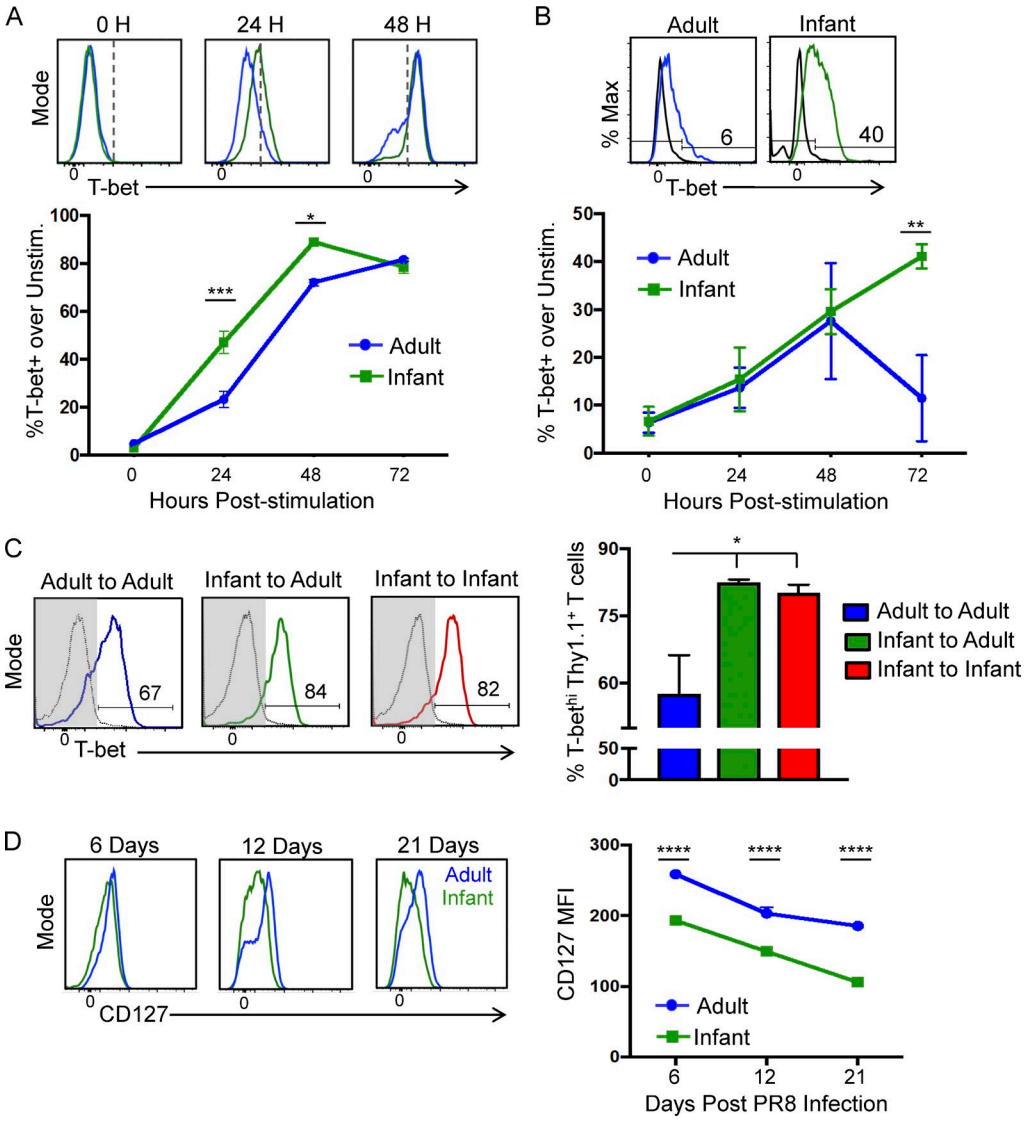

Figure 8. **Increased T-bet expression by mouse and human infant T cells in vivo and after in vitro activation.** (A) T-bet expression after in vitro activation of mouse infant or adult, naive ($CD44^{lo}$) $CD4^+$ T cells isolated from spleen. (Top) Representative flow cytometry histograms of T-bet expression after anti-CD3/anti-CD28 activation from 0 to 48 h. (Bottom) Percentages of stimulated adult or infant $CD4^+$ T cells expressing T-bet over unstimulated cells at indicated times ± SEM ($n = 3$ replicate samples/group/time point, derived from the spleens of 4–10 mice; representative of two experiments; significance determined by multiple Student's t tests with Welch's correction; *, $P < 0.05$; ***, $P < 0.001$). (B) T-bet expression in human infant and adult, naive ($CD45RO^-$) $CD4^+$ T cells from spleen (see Materials and methods) with or without stimulation. (Top) Representative flow cytometry histograms with percentages of $T\text{-}bet^{hi}$ T cells (expression over unstimulated) 72 h after activation with anti-CD3/anti-CD28 Abs by adult (blue) or infant (green) and unstimulated (Unstim.; black) cells at the indicated times. (Bottom) Percentages of stimulated adult or infant $CD4^+$ T cells expressing T-bet over unstimulated cells at indicated times ± SEM ($n = 4$ replicate samples/group/time point compiled from two independent experiments, with each group derived from a different spleen sample; significance determined by Student's t test; **, $P < 0.01$). (C) Augmented T-bet expression by infant influenza-specific $CD4^+$ T cells in vivo. (Left) Representative flow cytometry histograms with percentages of $T\text{-}bet^{hi}$ adult or infant HA T cells in the lungs of recipients at day 13 after PR8 influenza infection as in Fig. 6. (Right) Compiled percentages of adult or infant HA T cells in adult or infant recipient lung with a $T\text{-}bet^{hi}$ (expression over naive) phenotype ± SEM ($n = 3$–4 mice/group, compiled from two independent experiments; significance determined by one-way ANOVA with Holm-Sidak's multiple comparisons test; *, $P < 0.05$). (D) CD127 is reduced in infant compared with adult lung $CD4^+$ T cells after PR8 influenza infection. (Left) Representative flow cytometry histograms of CD127 expression by adult (blue) or infant (green) lung $CD4^+$ T cells at the indicated times after infection. (Right) Mean fluorescence intensity (MFI) values for CD127 expression by adult or infant lung $CD4^+$ T cells at the indicated times ± SEM ($n = 5$ mice/group per time point, compiled from three experiments; significance was determined by multiple Student's t tests with Welch's correction; ****, $P < 0.0001$).

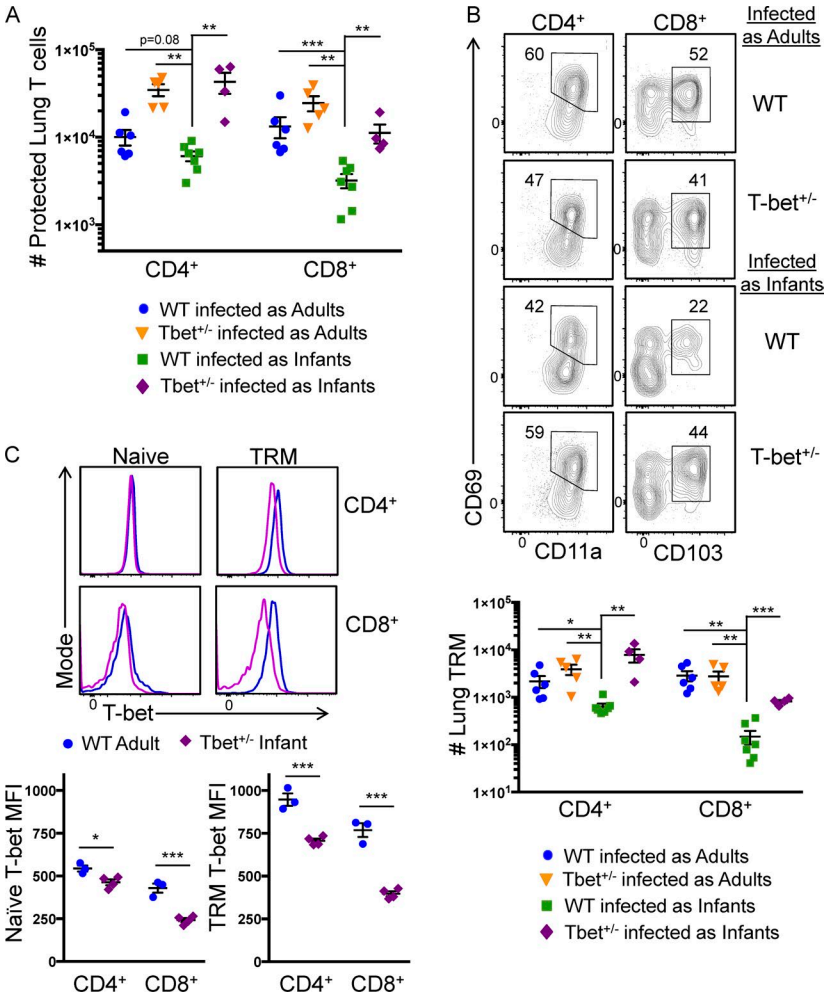

Figure 9. **Reduced T-bet expression in infant mice results in enhanced lung TRM establishment after influenza infection.** Adult and infant WT or age-matched T-bet$^{+/-}$ mice were infected with PR8 influenza, and lung T cells were analyzed 6–8 wk after infection. (A) Absolute numbers (±SEM) of lung CD4$^+$ and CD8$^+$ T cells protected from i.v. anti–Thy1 Abs ("protected"; Fig. 2) in WT or T-bet$^{+/-}$ mice infected 6–8 wk previously as adults (10–16 wk old) or as infants (2 wk old; n = 4–7 mice/group compiled from two independent experiments; significance was determined by multiple Student's t tests with Welch's correction; **, P < 0.01; ***, P < 0.001). (B) Expression of TRM phenotype markers (CD11a, CD69, CD103) by protected lung CD4$^+$ or CD8$^+$ T cells in WT or T-bet$^{+/-}$ mice previously infected as adults or infants as in A. (Top) Representative flow cytometry plots with percentages of CD11a and CD69 expression by CD4$^+$ (left) and CD69 and CD103 expression by CD8$^+$ (right) protected lung T cells. (Bottom) Absolute numbers (±SEM) of lung CD4$^+$ TRM (CD69$^+$CD11a$^+$) or CD8$^+$ TRM (CD69$^+$CD103$^+$) in WT and T-bet$^{+/-}$ mice previously infected as adults or infants (n = 4–7 mice/group compiled from two independent experiments; significance determined by multiple Student's t tests with Welch's correction; *, P < 0.05; **, P < 0.01; ***, P < 0.001). (C) T-bet expression by CD4$^+$ and CD8$^+$ naive and TRM subsets in previously infected WT adult mice or T-bet$^{+/-}$ infant mice. Graph (bottom) displays individual T-bet mean fluorescence intensity (MFI) values ± SEM for lung CD4$^+$ or CD8$^+$ naive or TRM T cells (n = 3–4 mice/group, representative of two independent experiments; significance determined by Student's t test with Welch's correction; *, P < 0.05; ***, P < 0.001).

et al., 2011; Sakai et al., 2014; Turner et al., 2014; Wu et al., 2014), which can also be generated by i.n. vaccination with bacille Calmette–Guérin or LAIV (Perdomo et al., 2016; Zens et al., 2016). We showed that, in multiple mouse strains and with different viral subtypes, infection or vaccination during infancy results in impaired TRM formation, as assessed by tissue localization and phenotype. Our findings are consistent with recent results using human organ-donor samples showing reduced CD103 expression by memory CD8$^+$ T cells isolated from infant lungs and intestines compared with memory CD8$^+$ T cells in adult mucosal sites (Thome et al., 2016). In response to heterosubtypic challenge, mice previously infected during infancy were less protected with reduced viral clearance compared with previously infected adults—particularly in FTY720-treated mice—when protection was limited to TRM. In untreated mice previously infected as infants, there was enhanced viral clearance to heterosubtypic challenge compared with naive mice, suggesting that infants may generate some circulating protective memory T cells, albeit in reduced numbers, compared with adults as also shown in an systemic viral infection model (Smith et al., 2014).

Reduced TRM generation during infant infection was intrinsic to infant T cells and was not a function of the infant lung environment as determined by adoptive transfer studies. The distinct transcriptional profile of infant (compared with adult) T cells migrating to the lung during infection included genes associated with migration, homing, differentiation, and cytokine responses, suggesting a distinct differentiation program for infant T cells. Notably, the gene expression pattern was enriched for T-bet–regulated genes, a master regulator for Th1 responses and effector cell differentiation (Szabo et al., 2000, 2002). Similarly, at very early times (24 h) after stimulation, infant T cells demonstrated a gene expression pattern enriched for molecules involved in cell cycle and proliferation consistent with enhanced T-bet expression. T-bet levels have been shown to control memory T cell generation with high levels of T-bet leading to terminal differentiation and cell death (Joshi et al., 2007) and intermediate expression of T-bet promoting TRM establishment (Laidlaw et al., 2014; Mackay et al., 2015).

We found that infant T cells in mice and humans exhibit greater up-regulation of T-bet expression after activation compared with adult T cells, suggesting that infant T cells are intrinsically programmed for terminal effector development.

Our results are consistent with findings that mouse, neonatal $CD8^+$ T cells exhibit increased proliferative expansion when stimulated (Smith et al., 2014), as do human cord-blood T cells (Schönland et al., 2003; Schüler et al., 2004)—features consistent with progression toward a terminal differentiation program. Infection of T-bet$^{+/-}$ infant mice expressing intermediate levels of T-bet, promoted TRM establishment at levels similar to that observed in both WT and T-bet$^{+/-}$ adults, suggesting a key role for that regulator in determining infant T cell fate.

Although the mechanisms underlying increased T-bet expression in infant T cells remain to be determined, the homeostatic expansion of T cells that occurs in early life (postnatally in mice and during fetal development in humans; Haynes et al., 1988) may be a contributing factor. In mice, homeostatic proliferation depends on mTOR signaling (Li et al., 2011), which, in turn, drives T-bet expression (Rao et al., 2010). The increased propensity for T-bet up-regulation may be a developmental adaptation for early life T cell responses. A major function of T-bet is to promote IFN-γ expression by binding to and remodeling the IFN-γ promoter locus (Mullen et al., 2001), which in neonatal T cells is hypermethylated and, therefore, less accessible to transcriptional up-regulation (White et al., 2002). Increased T-bet expression may be necessary to overcome transcriptional inhibition for promoting IFN-γ production (even at a low level) necessary for pathogen clearance to survive the critical period of early life, when generation of long-term protection is less pressing.

Our results have important implications for vaccine optimization in the early life period, to limit the global burden of disease. Although we demonstrate reduced generation of LAIV vaccine responses in infant, compared with adult, mice, particularly when assessing TRM formation, LAIV-vaccinated infants are better protected from heterosubtypic challenge than are IIV-vaccinated mice, suggesting that tissue-targeting is an optimal strategy for promoting early T cell responses. In humans, LAIV has previously shown to exhibit higher efficacy in children compared with adults (Belshe et al., 2007), and conversely, oral administration of vaccines during infancy has also proven efficacious. We propose that a combination of tissue targeting with modulation for promoting TRM responses may not only fortify in situ immunity during this vulnerable period but also generate long-term protective responses persisting throughout childhood and beyond.

MATERIALS AND METHODS

Mice

C57BL/6 or BALB/c mice were purchased (Charles River) or bred and maintained under specific pathogen–free conditions in a BSL2 biocontainment room within Columbia University Medical Center (CUMC) animal facilities. TS1 (HA TCR) mice (Kirberg et al., 1994) were bred and maintained within CUMC animal facilities. T-bet heterozygous mice were generated by crossing male *Tbx21*$^{-/-}$ mice (Intlekofer et al., 2005), provided by S. Reiner (Columbia Universtiy, New York, NY), with WT C57BL/6 females. To generate littermate controls, T-bet heterozygous males and females were crossed, and offspring were screened by PCR of genomic DNA extracted from ear punches using the Clontech Terra PCR Direct Polymerase Mix kit (Takara Bio Inc.) with the following primers: (1) forward, 5′-TATGATTACACTGCA GCTGTCTTCAG-3′; (2) WT reverse, 5′-CAGGAATGG GAACATTCGCCTGTG-3′; and (3) null reverse, 5′-CTC TGCCTCCCATCTCTTAGGAGC-3′. For all studies, infant mice were used between 10–14 d after birth, and adult mice were used between 8 and 20 wk of age, with both genders used. All animal studies and procedures were conducted according to the National Institutes of Health guidelines for the care and use of laboratory animals and were approved by the CUMC Institutional Animal Care and use Committee.

Acquisition of human splenocytes

Human splenic tissues were obtained from deceased (brain dead) organ donors at the time of organ acquisition for life-saving clinical transplantation through an approved protocol and material transfer agreement with LiveOnNY. Organ donors were free of chronic disease and cancer and were negative for HIV and hepatitis B and C. The study did not qualify as human subjects research, as confirmed by the Columbia University institutional review board because tissue samples were obtained from deceased individuals. Tissues were obtained and processed for single-cell suspensions, as previously described (Sathaliyawala et al., 2013; Thome et al., 2014, 2016).

Reagents

FluMist Quadrivalent, 2015–2016, live-attenuated vaccine (MedImmune) and Fluzone Quadrivalent, 2015–2016, inactivated virus vaccine (Sanofi Pasteur), both containing the four strains: (1) A/California/7/2009 (H1N1) pdm09, (2) A/Switzerland/9715293/2013 (H3N2), (3) B/Phuket/3073/2013, and (4) B/Brisbane/60/2008, were purchased from Moore Medical. Anti–CD3e (clone 145-2C11) and anti–CD28 (clone 37.51) mAbs were purchased as azide-free, low-endotoxin formulations from BD for use in T cell–activation assays. Fluorescently conjugated Abs for cell-surface phenotypic staining, cell sorting, and intracellular staining were purchased from BD, BioLegend, and eBioscience and are listed, including target, clone, color, and manufacturer, in Table S6. The influenza nucleoprotein-specific ($NP_{366–374}$ ASNENM DAM) MHCI H-$2D^b$ tetramer; the influenza, RNA-dependent RNA polymerase PB1 subunit-specific ($PB1_{703–711}$ SSY RRPVGI) MHCI H-$2K^b$ tetramer; and the influenza HA-specific ($HA_{533–541}$ IYSTVASSL) MHCI H-$2K^d$ tetramer, all conjugated to PE, were purchased from MBL International. FTY720 was purchased from Cayman Chemical.

Influenza virus infection

Mice were anesthetized by inhalation of isoflurane (5% induction/2% maintenance), delivered through a vaporizer within the CUMC animal facilities, and infected i.n. with weight-adjusted doses of PR8 (A/Puerto Rico/8/34 [H1N1]) or X31

(A/Hong Kong/1/68-x31 [H3N2]) influenza viruses. Appropriate viral doses were determined based on viral strain, mouse age and strain, and primary versus heterosubtypic infection, as listed in Table S7. Morbidity after infection was monitored by daily examination and weight assessment. Mice were euthanized when weight loss exceeded 30% of starting weight.

Vaccination

For vaccinations, adult and infant mice were administered 20 µl of FluMist (one tenth of the adult human dose) i.n. for a final dose of $10^{5.5–6.5}$ focus forming units/viral strain/mouse, or 50 µl of Fluzone (one tenth of the adult human dose) i.p. for a final dose of 1.5 µg HA/viral strain/animal.

FTY720 treatment

Mice were treated daily with 1 mg/kg FTY720 (25 µg/mouse) or PBS i.p., beginning 2–3 d before infection and continuing daily throughout infection.

In vivo antibody labeling and flow cytometry

For in vivo antibody labeling, mice were given 3 µg fluorochrome-conjugated anti–Thy1.2 or anti–CD45 Ab (Table S6) by i.v. injection 10 min before tissue harvest. Lungs were then perfused with 15–20 ml PBS via instillation of the right ventricle of the heart. Lungs and spleens were collected and lymphocytes isolated, as previously described. (Turner et al., 2014). Cells were stained with fluorochrome-conjugated Abs. To detect influenza-specific T cells, cells were incubated for an additional 30 min at room temperature (19–25°C) in the dark with a tetramer reagent and were analyzed using an LSRII flow cytometer (BD), and data were assessed using FlowJo software (Tree Star).

Viral titers

Influenza titers in lung homogenates were measured by a 50% tissue culture infective dose ($TCID_{50}$) assay, as previously described (Teijaro et al., 2010), with titers expressed as the reciprocal of the dilution of lung extract that corresponded to 50% virus growth in Madine–Darby canine kidney cells, as calculated by the Reed–Muench method.

Hemagglutination-inhibition assay

Serum-neutralizing Ab titers were measured by hemagglutination inhibition assay, as previously described (Teijaro et al., 2010). In brief, serum was collected by cardiac puncture, then treated overnight with Receptor Destroying Enzyme (Denka Seiken). Treated serum was serially diluted, incubated with PR8 or X31 whole virus particles as HA sources, then incubated with 0.5% chicken red blood cells (Lampire, Biological Laboratories). Titers were expressed as the reciprocal of the last dilution of serum that completely inhibited hemagglutination.

T cell activation studies

Naive ($CD44^{lo}$) $CD4^+$ T cells were enriched from mouse splenocytes using MagniSort $CD4^+$ naive T cell–negative selection kits (eBioscience). Human naive ($CD45RO^-$) $CD4^+$ T cells were purified from spleen using Mojosort naive T cell negative isolation kit (BioLegend). Purified, naive T cells (2×10^5) were activated for 24–72 h at 37°C in 96-well, flat-bottomed plates coated with a solution of 5 µg/ml anti-CD3 and 5 µg/ml anti-CD28. For intracellular staining, cells were first surface stained with Ab reagents and then fixed for 30 min at room temperature (19–25°C) in the dark with FoxP3 fixation/permeabilization buffer (eBioscience), washed with permeabilization buffer (eBioscience), and stained with fluorescently conjugated Abs to the transcription factor T-bet (Table S6) diluted in permeabilization buffer. Staining was performed for 30 min at room temperature (19–25°C) in the dark, followed by a minimum of 30 min at 4°C protected from light, before washing with FACS buffer.

T cell adoptive transfer

Naive $CD4^+$ T cells were isolated from the spleens of infant (10–14 d old) or adult (8–16 wk old) TS1 mice using the MagniSort $CD4^+$, naive T cell–enrichment kit (eBioscience), and $1.5–5 \times 10^5$ purified cells were transferred by i.p. injection into naive, congenic ($Thy1.2^+$) infant or adult recipients. The next day, recipient mice were infected i.n. with 10–13 $TCID_{50}$ PR8 influenza/g body weight (250–325 $TCID_{50}$ for adults and 70–91 $TCID_{50}$ for infants). For whole-transcriptome profiling studies, lungs were harvested 13 d after infection and processed as described for FACS analysis, and single-cell suspensions were stained with fluorescently conjugated Abs (Table S6). Transferred ($Thy1.1^+$) T cells were sorted with a BD Influx cell sorter, and sorted T cells were immediately pelleted and flash-frozen at −80°C until RNA extraction.

RNA isolation and RNA sequencing

RNA from sorted cells was isolated using the QIAGEN RNeasy Mini Kit, flash frozen, and stored at −80°C before quality analysis and library generation. Sample RNA integrity and concentration were assessed using an Agilent 2100 Bioanalyzer Instrument (Agilent Technologies), and all samples had RNA integrity number (RIN) values of ≥8. Library preparation and RNA sequencing were performed by the Columbia Genome Center using an Illumina HiSeq 2500 Instrument. RNA samples were sequenced in a single-read manner with a sequencing depth of 30 million reads. Mapping of reads to a mouse reference genome was performed with TopHat (Trapnell et al., 2009), with downstream estimation of gene abundance using cuff links (Trapnell et al., 2010). GEO accession number for RNA sequencing data: GSE101696.

Differential gene expression was determined using the R-based package DESeq2 (Love et al., 2014) available from Bioconductor (Huber et al., 2015). Gene expression heat maps were generated using Morpheus (http://software.broadinstitute.org/morpheus); with a p-value cutoff of 0.05 and sorting genes by log fold change (logFC). IPA software (QIAGEN) was used to predict upstream transcriptional regulators using all differentially expressed genes with a p-value

cutoff of 0.10. Transcriptional regulators were determined by selecting "transcriptional regulators" from the upstream regulators tab. Differentially expressed gene data were assessed for T-bet regulation by GSEA. A ranking statistic was computed for each gene that passed the default, independent, filtering criteria (Bourgon et al., 2010) of DESeq2 ($\alpha = 0.1$) by multiplying the log of its p-value with the sign of its logFC, and that ranked list was tested for enrichment of previously published T-bet–regulated gene sets (Zhu et al., 2012) by applying GSEA-preranked (Mootha et al., 2003) using a weighted scoring scheme and 1,000 permutations. GO data were evaluated using the protein–protein interaction database Search Tool for the Retrieval of Interacting Genes/Proteins (STRING; Szklarczyk et al., 2015) using the top 200 genes differentially expressed between infant and adult samples by logFC ($P < 0.05$).

Data analysis and visualization

Flow cytometry, weight loss, lung viral titer, and neutralizing Ab data were compiled and statistical analyses were performed using Prism software (GraphPad Software). Results are expressed as the mean value from individual groups ± SEM, unless otherwise designated, indicated by error bars. Significance between experimental groups was determined by one- or two-way ANOVA or the Student's *t* test and corrected for multiple comparisons, as indicated, assuming a normal distribution for all groups.

Online supplemental material

Table S1 shows up-regulated genes in infant versus adult primary HA effectors. Table S2 shows down-regulated genes in infant versus adult primary HA effectors. Table S3 shows up-regulated genes in 24-h–stimulated infant $CD4^+$ T cells. Table S4 shows down-regulated genes in 24-h–stimulated infant $CD4^+$ T cells. Table S5 provides GO terms for differentially expressed genes in 24-h–stimulated infant and adult $CD4^+$ T cells. Table S6 provides fluorophore-conjugated Abs used for flow cytometry. Table S7 provides the doses of influenza strain used in this study.

ACKNOWLEDGMENTS

We thank Esi Lamouse-Smith for assistance with influenza vaccines and Tomer Granot and Daniel Paik for critical reading of this manuscript.

This study was supported by National Institutes of Health grant R01 AI100119 awarded to D.L. Farber. K.D. Zens and M. Miron were supported by National Institutes of Health grant T32 AI106711 (principal investigator, D. Fidock). Research reported here was performed in the Columbia Center for Translational Immunology Flow Cytometry Core, supported in part by National Institutes of Health grants S10RR027050 and S10OD020056. The content is solely the responsibility of the authors and does not necessarily represent the official views of the National Institutes of Health.

The authors declare no competing financial interests.

Author contributions: K.D. Zens and D.L. Farber designed the research studies. K.D. Zens, J.K. Chen, R.S. Guyer, F. Cvetkovski, and M. Miron conducted experiments and analyzed data. F.L. Wu analyzed RNASeq data. K.D. Zens and D.L. Farber wrote the manuscript.

Submitted: 21 March 2017
Revised: 15 June 2017
Accepted: 3 August 2017

REFERENCES

Anderson, K.G., H. Sung, C.N. Skon, L. Lefrancois, A. Deisinger, V. Vezys, and D. Masopust. 2012. Cutting edge: Intravascular staining redefines lung CD8 T cell responses. *J. Immunol.* 189:2702–2706. http://dx.doi.org/10.4049/jimmunol.1201682

Anderson, K.G., K. Mayer-Barber, H. Sung, L. Beura, B.R. James, J.J. Taylor, L. Qunaj, T.S. Griffith, V. Vezys, D.L. Barber, and D. Masopust. 2014. Intravascular staining for discrimination of vascular and tissue leukocytes. *Nat. Protoc.* 9:209–222. http://dx.doi.org/10.1038/nprot.2014.005

Banerjee, A., S.M. Gordon, A.M. Intlekofer, M.A. Paley, E.C. Mooney, T. Lindsten, E.J. Wherry, and S.L. Reiner. 2010. Cutting edge: The transcription factor eomesodermin enables $CD8^+$ T cells to compete for the memory cell niche. *J. Immunol.* 185:4988–4992. http://dx.doi.org/10.4049/jimmunol.1002042

Belshe, R.B., K.M. Edwards, T. Vesikari, S.V. Black, R.E. Walker, M. Hultquist, G. Kemble, and E.M. Connor. CAIV-T Comparative Efficacy Study Group. 2007. Live attenuated versus inactivated influenza vaccine in infants and young children. *N. Engl. J. Med.* 356:685–696. http://dx.doi.org/10.1056/NEJMoa065368

Bevan, M.J. 2004. Helping the $CD8^+$ T-cell response. *Nat. Rev. Immunol.* 4:595–602. http://dx.doi.org/10.1038/nri1413

Bourgon, R., R. Gentleman, and W. Huber. 2010. Independent filtering increases detection power for high-throughput experiments. *Proc. Natl. Acad. Sci. USA.* 107:9546–9551. http://dx.doi.org/10.1073/pnas.0914005107

Cannarile, M.A., N.A. Lind, R. Rivera, A.D. Sheridan, K.A. Camfield, B.B. Wu, K.P. Cheung, Z. Ding, and A.W. Goldrath. 2006. Transcriptional regulator Id2 mediates $CD8^+$ T cell immunity. *Nat. Immunol.* 7:1317–1325. http://dx.doi.org/10.1038/ni1403

Chiba, K., Y. Yanagawa, Y. Masubuchi, H. Kataoka, T. Kawaguchi, M. Ohtsuki, and Y. Hoshino. 1998. FTY720, a novel immunosuppressant, induces sequestration of circulating mature lymphocytes by acceleration of lymphocyte homing in rats. I. FTY720 selectively decreases the number of circulating mature lymphocytes by acceleration of lymphocyte homing. *J. Immunol.* 160:5037–5044.

Connors, T.J., T.M. Ravindranath, K.L. Bickham, C.L. Gordon, F. Zhang, B. Levin, J.S. Baird, and D.L. Farber. 2016. Airway $CD8^+$ T cells are associated with lung injury during infant viral respiratory tract infection. *Am. J. Respir. Cell Mol. Biol.* 54:822–830. http://dx.doi.org/10.1165/rcmb.2015-0297OC

Crespo, M., D.G. Martinez, A. Cerissi, B. Rivera-Reyes, H.B. Bernstein, M.M. Lederman, S.F. Sieg, and A.A. Luciano. 2012. Neonatal T-cell maturation and homing receptor responses to Toll-like receptor ligands differ from those of adult naive T cells: Relationship to prematurity. *Pediatr. Res.* 71:136–143. http://dx.doi.org/10.1038/pr.2011.26

Dawson, T.C., M.A. Beck, W.A. Kuziel, F. Henderson, and N. Maeda. 2000. Contrasting effects of CCR5 and CCR2 deficiency in the pulmonary inflammatory response to influenza A virus. *Am. J. Pathol.* 156:1951–1959. http://dx.doi.org/10.1016/S0002-9440(10)65068-7

de Bree, G.J., E.M. van Leeuwen, T.A. Out, H.M. Jansen, R.E. Jonkers, and R.A. van Lier. 2005. Selective accumulation of differentiated $CD8^+$ T cells specific for respiratory viruses in the human lung. *J. Exp. Med.* 202:1433–1442. http://dx.doi.org/10.1084/jem.20051365

Garcia, A.M., S.A. Fadel, S. Cao, and M. Sarzotti. 2000. T cell immunity in neonates. *Immunol. Res.* 22:177–190. http://dx.doi.org/10.1385/IR:22:2-3:177

Gibbons, D., P. Fleming, A. Virasami, M.L. Michel, N.J. Sebire, K. Costeloe, R. Carr, N. Klein, and A. Hayday. 2014. Interleukin-8 (CXCL8) production

is a signatory T cell effector function of human newborn infants. *Nat. Med.* 20:1206–1210. http://dx.doi.org/10.1038/nm.3670

Graham, M.B., D.K. Dalton, D. Giltinan, V.L. Braciale, T.A. Stewart, and T.J. Braciale. 1993. Response to influenza infection in mice with a targeted disruption in the interferon-γ gene. *J. Exp. Med.* 178:1725–1732. http://dx.doi.org/10.1084/jem.178.5.1725

Graham, M.B., V.L. Braciale, and T.J. Braciale. 1994. Influenza virus-specific $CD4^+$ T helper type 2 T lymphocytes do not promote recovery from experimental virus infection. *J. Exp. Med.* 180:1273–1282. http://dx.doi.org/10.1084/jem.180.4.1273

Grindebacke, H., H. Stenstad, M. Quiding-Järbrink, J. Waldenström, I. Adlerberth, A.E. Wold, and A. Rudin. 2009. Dynamic development of homing receptor expression and memory cell differentiation of infant $CD4^+CD25^{high}$ regulatory T cells. *J. Immunol.* 183:4360–4370. http://dx.doi.org/10.4049/jimmunol.0901091

Haynes, B.F., M.E. Martin, H.H. Kay, and J. Kurtzberg. 1988. Early events in human T cell ontogeny. Phenotypic characterization and immunohistologic localization of T cell precursors in early human fetal tissues. *J. Exp. Med.* 168:1061–1080. http://dx.doi.org/10.1084/jem.168.3.1061

Huber, W., V.J. Carey, R. Gentleman, S. Anders, M. Carlson, B.S. Carvalho, H.C. Bravo, S. Davis, L. Gatto, T. Girke, et al. 2015. Orchestrating high-throughput genomic analysis with Bioconductor. *Nat. Methods.* 12:115–121. http://dx.doi.org/10.1038/nmeth.3252

Intlekofer, A.M., N. Takemoto, E.J. Wherry, S.A. Longworth, J.T. Northrup, V.R. Palanivel, A.C. Mullen, C.R. Gasink, S.M. Kaech, J.D. Miller, et al. 2005. Effector and memory $CD8^+$ T cell fate coupled by T-bet and eomesodermin. *Nat. Immunol.* 6:1236–1244. http://dx.doi.org/10.1038/ni1268

Intlekofer, A.M., N. Takemoto, C. Kao, A. Banerjee, F. Schambach, J.K. Northrop, H. Shen, E.J. Wherry, and S.L. Reiner. 2007. Requirement for T-bet in the aberrant differentiation of unhelped memory CD8+ T cells. *J. Exp. Med.* 204:2015–2021. http://dx.doi.org/10.1084/jem.20070841

Jelley-Gibbs, D.M., D.M. Brown, J.P. Dibble, L. Haynes, S.M. Eaton, and S.L. Swain. 2005. Unexpected prolonged presentation of influenza antigens promotes CD4 T cell memory generation. *J. Exp. Med.* 202:697–706. http://dx.doi.org/10.1084/jem.20050227

Ji, Y., Z. Pos, M. Rao, C.A. Klebanoff, Z. Yu, M. Sukumar, R.N. Reger, D.C. Palmer, Z.A. Borman, P. Muranski, et al. 2011. Repression of the DNA-binding inhibitor Id3 by Blimp-1 limits the formation of memory $CD8^+$ T cells. *Nat. Immunol.* 12:1230–1237. http://dx.doi.org/10.1038/ni.2153

Jiang, X., R.A. Clark, L. Liu, A.J. Wagers, R.C. Fuhlbrigge, and T.S. Kupper. 2012. Skin infection generates non-migratory memory $CD8^+$ T(RM) cells providing global skin immunity. *Nature.* 483:227–231. http://dx.doi.org/10.1038/nature10851

Johnston, R.J., A.C. Poholek, D. DiToro, I. Yusuf, D. Eto, B. Barnett, A.L. Dent, J. Craft, and S. Crotty. 2009. Bcl6 and Blimp-1 are reciprocal and antagonistic regulators of T follicular helper cell differentiation. *Science.* 325:1006–1010. http://dx.doi.org/10.1126/science.1175870

Joshi, N.S., W. Cui, A. Chandele, H.K. Lee, D.R. Urso, J. Hagman, L. Gapin, and S.M. Kaech. 2007. Inflammation directs memory precursor and short-lived effector $CD8^+$ T cell fates via the graded expression of T-bet transcription factor. *Immunity.* 27:281–295. http://dx.doi.org/10.1016/j.immuni.2007.07.010

Kaech, S.M., J.T. Tan, E.J. Wherry, B.T. Konieczny, C.D. Surh, and R. Ahmed. 2003. Selective expression of the interleukin 7 receptor identifies effector CD8 T cells that give rise to long-lived memory cells. *Nat. Immunol.* 4:1191–1198. http://dx.doi.org/10.1038/ni1009

Kirberg, J., A. Baron, S. Jakob, A. Rolink, K. Karjalainen, and H. von Boehmer. 1994. Thymic selection of $CD8^+$ single positive cells with a class II major histocompatibility complex-restricted receptor. *J. Exp. Med.* 180:25–34. http://dx.doi.org/10.1084/jem.180.1.25

Knox, J.J., G.L. Cosma, M.R. Betts, and L.M. McLane. 2014. Characterization of T-bet and eomes in peripheral human immune cells. *Front. Immunol.* 5:217 (published erratum appears in *Front. Immunol.* 2016. 7:337). http://dx.doi.org/10.3389/fimmu.2014.00217

Kohlmeier, J.E., S.C. Miller, J. Smith, B. Lu, C. Gerard, T. Cookenham, A.D. Roberts, and D.L. Woodland. 2008. The chemokine receptor CCR5 plays a key role in the early memory $CD8^+$ T cell response to respiratory virus infections. *Immunity.* 29:101–113. http://dx.doi.org/10.1016/j.immuni.2008.05.011

Krämer, A., J. Green, J. Pollard Jr., and S. Tugendreich. 2014. Causal analysis approaches in Ingenuity Pathway Analysis. *Bioinformatics.* 30:523–530. http://dx.doi.org/10.1093/bioinformatics/btt703

Laidlaw, B.J., N. Zhang, H.D. Marshall, M.M. Staron, T. Guan, Y. Hu, L.S. Cauley, J. Craft, and S.M. Kaech. 2014. $CD4^+$ T cell help guides formation of $CD103^+$ lung-resident memory $CD8^+$ T cells during influenza viral infection. *Immunity.* 41:633–645. http://dx.doi.org/10.1016/j.immuni.2014.09.007

Le Campion, A., C. Bourgeois, F. Lambolez, B. Martin, S. Léaument, N. Dautigny, C. Tanchot, C. Pénit, and B. Lucas. 2002. Naive T cells proliferate strongly in neonatal mice in response to self-peptide/self-MHC complexes. *Proc. Natl. Acad. Sci. USA.* 99:4538–4543. http://dx.doi.org/10.1073/pnas.062621699

Lee, L.N., E.O. Ronan, C. de Lara, K.L. Franken, T.H. Ottenhoff, E.Z. Tchilian, and P.C. Beverley. 2011. CXCR6 is a marker for protective antigen-specific cells in the lungs after intranasal immunization against *Mycobacterium tuberculosis*. *Infect. Immun.* 79:3328–3337. http://dx.doi.org/10.1128/IAI.01133-10

Lewis, D.B., A. Larsen, and C.B. Wilson. 1986. Reduced interferon-γ mRNA levels in human neonates. Evidence for an intrinsic T cell deficiency independent of other genes involved in T cell activation. *J. Exp. Med.* 163:1018–1023. http://dx.doi.org/10.1084/jem.163.4.1018

Lewis, D.B., C.C. Yu, J. Meyer, B.K. English, S.J. Kahn, and C.B. Wilson. 1991. Cellular and molecular mechanisms for reduced interleukin 4 and interferon-γ production by neonatal T cells. *J. Clin. Invest.* 87:194–202. http://dx.doi.org/10.1172/JCI114970

Li, Q., R.R. Rao, K. Araki, K. Pollizzi, K. Odunsi, J.D. Powell, and P.A. Shrikant. 2011. A central role for mTOR kinase in homeostatic proliferation induced $CD8^+$ T cell memory and tumor immunity. *Immunity.* 34:541–553. http://dx.doi.org/10.1016/j.immuni.2011.04.006

Lines, J.L., S. Hoskins, M. Hollifield, L.S. Cauley, and B.A. Garvy. 2010. The migration of T cells in response to influenza virus is altered in neonatal mice. *J. Immunol.* 185:2980–2988. http://dx.doi.org/10.4049/jimmunol.0903075

Love, M.I., W. Huber, and S. Anders. 2014. Moderated estimation of fold change and dispersion for RNA-seq data with DESeq2. *Genome Biol.* 15:550. http://dx.doi.org/10.1186/s13059-014-0550-8

Mackay, L.K., E. Wynne-Jones, D. Freestone, D.G. Pellicci, L.A. Mielke, D.M. Newman, A. Braun, F. Masson, A. Kallies, G.T. Belz, and F.R. Carbone. 2015. T-box transcription factors combine with the cytokines TGF-β and IL-15 to control tissue-resident memory T cell fate. *Immunity.* 43:1101–1111. http://dx.doi.org/10.1016/j.immuni.2015.11.008

Masopust, D., J. Jiang, H. Shen, and L. Lefrançois. 2001. Direct analysis of the dynamics of the intestinal mucosa CD8 T cell response to systemic virus infection. *J. Immunol.* 166:2348–2356. http://dx.doi.org/10.4049/jimmunol.166.4.2348

Min, B., R. McHugh, G.D. Sempowski, C. Mackall, G. Foucras, and W.E. Paul. 2003. Neonates support lymphopenia-induced proliferation. *Immunity.* 18:131–140. http://dx.doi.org/10.1016/S1074-7613(02)00508-3

Mootha, V.K., C.M. Lindgren, K.F. Eriksson, A. Subramanian, S. Sihag, J. Lehar, P. Puigserver, E. Carlsson, M. Ridderstråle, E. Laurila, et al. 2003. PGC-1α-responsive genes involved in oxidative phosphorylation are coordinately downregulated in human diabetes. *Nat. Genet.* 34:267–273. http://dx.doi.org/10.1038/ng1180

Morgan, A.J., C. Guillen, F.A. Symon, S.S. Birring, J.J. Campbell, and A.J. Wardlaw. 2008. CXCR6 identifies a putative population of retained human lung T cells characterised by co-expression of activation markers. *Immunobiology.* 213:599–608. http://dx.doi.org/10.1016/j.imbio.2008.01.005

Mueller, S.N., T. Gebhardt, F.R. Carbone, and W.R. Heath. 2013. Memory T cell subsets, migration patterns, and tissue residence. *Annu. Rev. Immunol.* 31:137–161. http://dx.doi.org/10.1146/annurev-immunol-032712-095954

Mullen, A.C., F.A. High, A.S. Hutchins, H.W. Lee, A.V. Villarino, D.M. Livingston, A.L. Kung, N. Cereb, T.P. Yao, S.Y. Yang, and S.L. Reiner. 2001. Role of T-bet in commitment of TH1 cells before IL-12-dependent selection. *Science.* 292:1907–1910. http://dx.doi.org/10.1126/science.1059835

Perdomo, C., U. Zedler, A.A. Kühl, L. Lozza, P. Saikali, L.E. Sander, A. Vogelzang, S.H. Kaufmann, and A. Kupz. 2016. Mucosal BCG vaccination induces protective lung-resident memory T cell populations against tuberculosis. *MBio.* 7:e01686-16. http://dx.doi.org/10.1128/mBio.01686-16

Pinschewer, D.D., A.F. Ochsenbein, B. Odermatt, V. Brinkmann, H. Hengartner, and R.M. Zinkernagel. 2000. FTY720 immunosuppression impairs effector T cell peripheral homing without affecting induction, expansion, and memory. *J. Immunol.* 164:5761–5770. http://dx.doi.org/10.4049/jimmunol.164.11.5761

PrabhuDas, M., B. Adkins, H. Gans, C. King, O. Levy, O. Ramilo, and C.A. Siegrist. 2011. Challenges in infant immunity: Implications for responses to infection and vaccines. *Nat. Immunol.* 12:189–194. http://dx.doi.org/10.1038/ni0311-189

Purwar, R., J. Campbell, G. Murphy, W.G. Richards, R.A. Clark, and T.S. Kupper. 2011. Resident memory T cells (T_{RM}) are abundant in human lung: Diversity, function, and antigen specificity. *PLoS One.* 6:e16245. http://dx.doi.org/10.1371/journal.pone.0016245

Rao, R.R., Q. Li, K. Odunsi, and P.A. Shrikant. 2010. The mTOR kinase determines effector versus memory $CD8^+$ T cell fate by regulating the expression of transcription factors T-bet and eomesodermin. *Immunity.* 32:67–78. http://dx.doi.org/10.1016/j.immuni.2009.10.010

Ray, S.J., S.N. Franki, R.H. Pierce, S. Dimitrova, V. Koteliansky, A.G. Sprague, P.C. Doherty, A.R. de Fougerolles, and D.J. Topham. 2004. The collagen binding α1β1 integrin VLA-1 regulates CD8 T cell-mediated immune protection against heterologous influenza infection. *Immunity.* 20:167–179. http://dx.doi.org/10.1016/S1074-7613(04)00021-4

Richter, M., S.J. Ray, T.J. Chapman, S.J. Austin, J. Rebhahn, T.R. Mosmann, H. Gardner, V. Kotelianski, A.R. deFougerolles, and D.J. Topham. 2007. Collagen distribution and expression of collagen-binding α1β1 (VLA-1) and α2β1 (VLA-2) integrins on CD4 and CD8 T cells during influenza infection. *J. Immunol.* 178:4506–4516. http://dx.doi.org/10.4049/jimmunol.178.7.4506

Sakai, S., K.D. Kauffman, J.M. Schenkel, C.C. McBerry, K.D. Mayer-Barber, D. Masopust, and D.L. Barber. 2014. Cutting edge: Control of *Mycobacterium tuberculosis* infection by a subset of lung parenchyma-homing CD4 T cells. *J. Immunol.* 192:2965–2969. http://dx.doi.org/10.4049/jimmunol.1400019

Sathaliyawala, T., M. Kubota, N. Yudanin, D. Turner, P. Camp, J.J. Thome, K.L. Bickham, H. Lerner, M. Goldstein, M. Sykes, et al. 2013. Distribution and compartmentalization of human circulating and tissue-resident memory T cell subsets. *Immunity.* 38:187–197. http://dx.doi.org/10.1016/j.immuni.2012.09.020

Schluns, K.S., W.C. Kieper, S.C. Jameson, and L. Lefrançois. 2000. Interleukin-7 mediates the homeostasis of naïve and memory CD8 T cells in vivo. *Nat. Immunol.* 1:426–432. http://dx.doi.org/10.1038/80868

Schönland, S.O., J.K. Zimmer, C.M. Lopez-Benitez, T. Widmann, K.D. Ramin, J.J. Goronzy, and C.M. Weyand. 2003. Homeostatic control of T-cell generation in neonates. *Blood.* 102:1428–1434. http://dx.doi.org/10.1182/blood-2002-11-3591

Schüler, T., G.J. Hämmerling, and B. Arnold. 2004. Cutting edge: IL-7-dependent homeostatic proliferation of $CD8^+$ T cells in neonatal mice allows the generation of long-lived natural memory T cells. *J. Immunol.* 172:15–19. http://dx.doi.org/10.4049/jimmunol.172.1.15

Shin, H., and A. Iwasaki. 2012. A vaccine strategy that protects against genital herpes by establishing local memory T cells. *Nature.* 491:463–467. http://dx.doi.org/10.1038/nature11522

Siegrist, C.A. 2007. The challenges of vaccine responses in early life: Selected examples. *J. Comp. Pathol.* 137(Suppl 1):S4–S9. http://dx.doi.org/10.1016/j.jcpa.2007.04.004

Smith, N.L., E. Wissink, J. Wang, J.F. Pinello, M.P. Davenport, A. Grimson, and B.D. Rudd. 2014. Rapid proliferation and differentiation impairs the development of memory $CD8^+$ T cells in early life. *J. Immunol.* 193:177–184. http://dx.doi.org/10.4049/jimmunol.1400553

Subramanian, A., P. Tamayo, V.K. Mootha, S. Mukherjee, B.L. Ebert, M.A. Gillette, A. Paulovich, S.L. Pomeroy, T.R. Golub, E.S. Lander, and J.P. Mesirov. 2005. Gene set enrichment analysis: a knowledge-based approach for interpreting genome-wide expression profiles. *Proc. Natl. Acad. Sci. USA.* 102:15545–15550. http://dx.doi.org/10.1073/pnas.0506580102

Sun, J.C., and M.J. Bevan. 2003. Defective CD8 T cell memory following acute infection without CD4 T cell help. *Science.* 300:339–342. http://dx.doi.org/10.1126/science.1083317

Surh, C.D., and J. Sprent. 2000. Homeostatic T cell proliferation: How far can T cells be activated to self-ligands? *J. Exp. Med.* 192:F9–F14. http://dx.doi.org/10.1084/jem.192.4.F9

Surh, C.D., and J. Sprent. 2008. Homeostasis of naive and memory T cells. *Immunity.* 29:848–862. http://dx.doi.org/10.1016/j.immuni.2008.11.002

Szabo, S.J., S.T. Kim, G.L. Costa, X. Zhang, C.G. Fathman, and L.H. Glimcher. 2000. A novel transcription factor, T-bet, directs Th1 lineage commitment. *Cell.* 100:655–669. http://dx.doi.org/10.1016/S0092-8674(00)80702-3

Szabo, S.J., B.M. Sullivan, C. Stemmann, A.R. Satoskar, B.P. Sleckman, and L.H. Glimcher. 2002. Distinct effects of T-bet in TH1 lineage commitment and IFN-γ production in CD4 and CD8 T cells. *Science.* 295:338–342. http://dx.doi.org/10.1126/science.1065543

Szklarczyk, D., A. Franceschini, S. Wyder, K. Forslund, D. Heller, J. Huerta-Cepas, M. Simonovic, A. Roth, A. Santos, K.P. Tsafou, et al. 2015. STRING v10: Protein–protein interaction networks, integrated over the tree of life. *Nucleic Acids Res.* 43(D1):D447–D452. http://dx.doi.org/10.1093/nar/gku1003

Teijaro, J.R., D. Verhoeven, C.A. Page, D. Turner, and D.L. Farber. 2010. Memory CD4 T cells direct protective responses to influenza virus in the lungs through helper-independent mechanisms. *J. Virol.* 84:9217–9226. http://dx.doi.org/10.1128/JVI.01069-10

Teijaro, J.R., D. Turner, Q. Pham, E.J. Wherry, L. Lefrançois, and D.L. Farber. 2011. Cutting edge: Tissue-retentive lung memory CD4 T cells mediate optimal protection to respiratory virus infection. *J. Immunol.* 187:5510–5514. http://dx.doi.org/10.4049/jimmunol.1102243

Thieu, V.T., Q. Yu, H.C. Chang, N. Yeh, E.T. Nguyen, S. Sehra, and M.H. Kaplan. 2008. Signal transducer and activator of transcription 4 is required for the transcription factor T-bet to promote T helper 1 cell-fate determination. *Immunity.* 29:679–690. http://dx.doi.org/10.1016/j.immuni.2008.08.017

Thome, J.J., N. Yudanin, Y. Ohmura, M. Kubota, B. Grinshpun, T. Sathaliyawala, T. Kato, H. Lerner, Y. Shen, and D.L. Farber. 2014. Spatial map of human T cell compartmentalization and maintenance over decades of life. *Cell.* 159:814–828. http://dx.doi.org/10.1016/j.cell.2014.10.026

Thome, J.J., K.L. Bickham, Y. Ohmura, M. Kubota, N. Matsuoka, C. Gordon, T. Granot, A. Griesemer, H. Lerner, T. Kato, and D.L. Farber. 2016. Early-life compartmentalization of human T cell differentiation and regulatory

function in mucosal and lymphoid tissues. *Nat. Med.* 22:72–77. http://dx.doi.org/10.1038/nm.4008

Trapnell, C., L. Pachter, and S.L. Salzberg. 2009. TopHat: Discovering splice junctions with RNA-Seq. *Bioinformatics.* 25:1105–1111. http://dx.doi.org/10.1093/bioinformatics/btp120

Trapnell, C., B.A. Williams, G. Pertea, A. Mortazavi, G. Kwan, M.J. van Baren, S.L. Salzberg, B.J. Wold, and L. Pachter. 2010. Transcript assembly and quantification by RNA-Seq reveals unannotated transcripts and isoform switching during cell differentiation. *Nat. Biotechnol.* 28:511–515. http://dx.doi.org/10.1038/nbt.1621

Turner, D.L., and D.L. Farber. 2014. Mucosal resident memory CD4 T cells in protection and immunopathology. *Front. Immunol.* 5:331. http://dx.doi.org/10.3389/fimmu.2014.00331

Turner, D.L., K.L. Bickham, J.J. Thome, C.Y. Kim, F. D'Ovidio, E.J. Wherry, and D.L. Farber. 2014. Lung niches for the generation and maintenance of tissue-resident memory T cells. *Mucosal Immunol.* 7:501–510. http://dx.doi.org/10.1038/mi.2013.67

Wakim, L.M., A. Woodward-Davis, and M.J. Bevan. 2010. Memory T cells persisting within the brain after local infection show functional adaptations to their tissue of residence. *Proc. Natl. Acad. Sci. USA.* 107:17872–17879. http://dx.doi.org/10.1073/pnas.1010201107

White, G.P., P.M. Watt, B.J. Holt, and P.G. Holt. 2002. Differential patterns of methylation of the IFN-gamma promoter at CpG and non-CpG sites underlie differences in IFN-γ gene expression between human neonatal and adult CD45RO$^-$ T cells. *J. Immunol.* 168:2820–2827. http://dx.doi.org/10.4049/jimmunol.168.6.2820

Williams, M.A., B.J. Holmes, J.C. Sun, and M.J. Bevan. 2006. Developing and maintaining protective CD8$^+$ memory T cells. *Immunol. Rev.* 211:146–153. http://dx.doi.org/10.1111/j.0105-2896.2006.00389.x

Wu, T., Y. Hu, Y.T. Lee, K.R. Bouchard, A. Benechet, K. Khanna, and L.S. Cauley. 2014. Lung-resident memory CD8 T cells (TRM) are indispensable for optimal cross-protection against pulmonary virus infection. *J. Leukoc. Biol.* 95:215–224. http://dx.doi.org/10.1189/jlb.0313180

Yang, C.Y., J.A. Best, J. Knell, E. Yang, A.D. Sheridan, A.K. Jesionek, H.S. Li, R.R. Rivera, K.C. Lind, L.M. D'Cruz, et al. 2011. The transcriptional regulators Id2 and Id3 control the formation of distinct memory CD8$^+$ T cell subsets. *Nat. Immunol.* 12:1221–1229. http://dx.doi.org/10.1038/ni.2158

You, D., M. Ripple, S. Balakrishna, D. Troxclair, D. Sandquist, L. Ding, T.A. Ahlert, and S.A. Cormier. 2008. Inchoate CD8$^+$ T cell responses in neonatal mice permit influenza-induced persistent pulmonary dysfunction. *J. Immunol.* 181:3486–3494. http://dx.doi.org/10.4049/jimmunol.181.5.3486

Zens, K.D., J.-K. Chen, and D.L. Farber. 2016. Vaccine-generated lung tissue-resident memory T cells provide heterosubtypic protection to influenza infection. *JCI Insight.* 1:e85832. http://dx.doi.org/10.1172/jci.insight.85832

Zhu, J., D. Jankovic, A.J. Oler, G. Wei, S. Sharma, G. Hu, L. Guo, R. Yagi, H. Yamane, G. Punkosdy, et al. 2012. The transcription factor T-bet is induced by multiple pathways and prevents an endogenous Th2 cell program during Th1 cell responses. *Immunity.* 37:660–673. http://dx.doi.org/10.1016/j.immuni.2012.09.007